1 **The terrestrial landscapes of tetrapod evolution in earliest Carboniferous**

2 **seasonal wetlands of SE Scotland**

3 Timothy I. Kearsey[a]*, Carys E. Bennett[b], David Millward[a], Sarah J. Davies[b], Charles J. B.

4 Gowing [c], Simon J. Kemp[c], Melanie J. Leng[d], John E. A. Marshall[e], Michael A. E. Browne[a]

5 *[a] British Geological Survey, Lyell Centre, Research Avenue South, Riccarton, Edinburgh, EH14 4AP*

6 *[b] Department of Geology, University of Leicester, Leicester, LE1 7RH*

7 *[c] British Geological Survey, Environmental Science Centre, Keyworth, Nottingham, NG12 5GG*

8 *[d]NERC Isotope Geosciences Facilities, British Geological Survey, Keyworth, Nottingham, NG12 5GG*

9 *[d] Ocean and Earth Science, National Oceanography Centre, Southampton, University of Southampton, SO14*

10 *3ZH*

11 **corresponding author:timk1@bgs.ac.uk*

12

13 **ABSTRACT**

14 The Lower Mississippian (Tournaisian) Ballagan Formation in SE Scotland yields tetrapod
15 fossils that provide fresh insights into the critical period when these animals first moved onto
16 land. The key to understanding the palaeoenvironments where they lived is a detailed analysis
17 of the sedimentary architecture of this formation, one of the thickest and most completely
18 documented examples of a coastal floodplain and marginal marine succession from this
19 important transitional time anywhere in the world. Palaeosols are abundant, providing a
20 unique insight into the early Carboniferous habitats and climate.

21 More than 200 separate palaeosols are described from three sections through the formation.
22 The palaeosols range in thickness from 0.02 to 1.85 m and are diverse: most are Entisols and
23 Inceptisols (63%), indicating relatively brief periods of soil development. Gleyed Inseptisols
24 and Vertisols are less common (37%). Vertisols are the thickest palaeosols (up to 185 cm) in
25 the Ballagan Formation and have common vertic cracks. Roots are abundant through all the
26 palaeosols, from shallow mats and thin hair-like traces to sporadic thicker root traces typical
27 of arborescent lycopods.

28 Geochemical, isotope and clay mineralogical analyses of the palaeosols indicate a range in
29 soil alkalinity and amount of water logging. Estimates of mean annual rainfall from palaeosol
30 compositions are 1000 –1500 mm per year. The high mean annual rainfall and variable soil
31 alkalinities contrast markedly with dry periods that developed deep penetrating cracks and
32 evaporite deposits. It is concluded that during the early Carboniferous, this region
33 experienced a sharply contrasting seasonal climate and that the floodplain hosted a mosaic of
34 closely juxtaposed but distinct habitats in which the tetrapods lived. The diversification of

coastal floodplain environments identified here may link to the evolution and movement of tetrapods into the terrestrial realm.

1. Introduction

The terrestrialization of vertebrates is one of the most important events in the evolution of life on Earth. Fundamental to understanding what drove evolution along this pathway is characterization of the subaerial environment in which the first dominantly terrestrial tetrapods lived. Around the world a wide range of Mid to Late Devonian taxa and trackways document the earliest phases of limbed vertebrate evolution from fishes (Clack, 1997; Narkiewicz and Ahlberg, 2010; Pierce et al. 2012; Narkiewicz et al., 2015; Lucas, 2015). In Poland, the occurrence of Mid Devonian tetrapod trackways suggests this change may have been driven by the development of novel habitats such as woodlands (Retallack, 2011) and intertidal and lagoonal environments (Niedzwiedzki et al., 2010). However, these early forms of limbed vertebrates have been shown to be mainly aquatic or semi-aquatic, with primitive features (Clack, 2009; Pierce et al., 2012; Smithson et al., 2012) and the trackways were formed underwater (Narkiewicz et al., 2015). This suggests that the Mid to Late Devonian tetrapods lacked terrestrial capability (Lucas, 2015). By the mid-Visean, the first evidence of fully terrestrial tetrapods is found in the Midland Valley of Scotland (Paton et al., 1999). The time between the mid-Visean tetrapod discoveries and Devonian tetrapods has been termed 'Romer's Gap' due to the lack of tetrapod fossil material found during this interval (Clack, 2002). The cause of this gap has been attributed to environmental factors such as a low atmospheric oxygen content in the Tournaisian (Ward et al., 2006) or the move of tetrapods to woodlands with poor preservation potential (Retallack, 2011).

60   Recent discoveries from the Tournaisian of SE Scotland and Nova Scotia have started

61   to fill Romer's Gap (Smithson et al., 2012; Anderson et al., 2015). Tetrapods from these

62   localities include both terrestrial and aquatic forms suggesting that full terrestrialization of

63   tetrapods occurred soon after the Late-Devonian mass-extinction event (Kaiser et al., 2015).

64   Garcia et al. (2006) have suggested that one of the factors that may have driven tetrapod

65   diversification was the evolution in the early Carboniferous of a wealth of new habitats, and

66   by implication palaeosols, suitable for continental organisms.

67   Palaeosols are one of the few direct indicators of the subaerial part of the floodplain

68   (Retallack, 1993; Sheldon and Tabor, 2009) and provide a direct record of changes in climate

69   and landscape architecture. Furthermore, they can also be used as proxies for estimating

70   palaeo-rainfall and atmospheric variability (Sheldon and Tabor, 2009; Nordt and Driese,

71   2010; Retallack and Huang, 2011). Both Anderton (1985) and Williams et al. (2005)

72   identified palaeosols in the Tournaisian Ballagan Formation in SE Scotland which hosts the

73   new tetrapod discoveries (Smithson et al., 2012). They did not, however, provide a detailed

74   nor systematic description and thus under-estimated palaeosol frequency and diversity. Here

75   we describe and interpret for the first time the palaeosols found in the Ballagan Formation, in

76   order to understand the range of habitats available to the earliest terrestrial tetrapods.

77   **2. Geological setting**

78   The Ballagan Formation crops out through the Midland Valley of Scotland and in the

79   north of England (Figs. 1, 2). Previously known as the lower part of the Calciferous

80   Sandstone Measures in the Midland Valley and as the Cementstone Group in northern

81   England, the Ballagan Formation overlies the Kinnesswood Formation, a succession of

82   fluvial sandstone beds with many rhizocretions (Browne et al., 1999; Scott, 1986). Previous

83   studies have suggested that the Ballagan Formation was deposited on a low-lying coastal

84 floodplain (Anderton, 1985; Andrews and Nabi, 1998; Andrews et al., 1991; Scott, 1986;

85 Stephenson et al., 2002, 2004a; Turner, 1991). The formation comprises grey siltstone which

86 is reddened in parts, along with sporadic nodules and many thin beds of ferroan dolostone,

87 averaging 30 cm thick, and locally known as 'cementstones' (Belt et al., 1967). Bennett et al.

88 (2016) identified ten facies and three facies associations, the latter comprising a fluvial facies

89 association, an overbank facies association and a saline-hypersaline lake facies association.

90 Parts of the Ballagan Formation, where ferroan dolostone beds are common, also contain thin

91 beds or nodules of gypsum and/or anhydrite and, in some sections, rare siltstone

92 pseudomorphs after halite (Scott, 1986). All the fine-grained sedimentary rocks in the

93 Ballagan Formation also contain desiccation cracks indicating periodic drying out of the

94 substrate.

95   In SE Scotland and neighbouring northern England the succession includes units, 5-30

96 m thick, of fine- and medium-grained sandstone, containing trough cross-bedding and lateral

97 accretion surfaces. Thin, conglomerate lags commonly occur at the base of units interpreted

98 as meandering fluvial channel systems (Scott, 1986). Palaeosols and rooted horizons have

99 been identified previously in the Ballagan Formation, some of which appear to be associated

100 with the cementstone units (Anderton, 1985; Andrews et al., 1991; Scott, 1986; Turner,

101 1991). Pedogenic calcrete occurs in the uppermost part of the formation in the Cockburnspath

102 outlier near Dunbar on the East Lothian coast (Andrews and Nabi, 1998) although it has not

103 been identified elsewhere.

104   The Ballagan Formation is predominantly Tournaisian in age and falls mostly in the

105 CM palynozone (Stephenson et al., 2002; Stephenson et al., 2004a, b; Williams et al., 2005).

106 At Burnmouth the lowest beds in the formation have yielded miospores of the VI palynozone

107 at the base of the Tournaisian (Smithson et al., 2012) (Fig. 2).

3. Materials and methods

109 *3.1. Localities*

110   In SE Scotland the Ballagan Formation is generally very poorly exposed, except for

111   coastal sections such as the foreshore at Burnmouth, which forms the first of three sections

112   considered here (Fig. 1). The foreshore and cliff section at Burnmouth (British National Grid

113   NT 95797 60944) is a 520 m thick section of vertically dipping strata that extends from the

114   base to the top of the Ballagan Formation. The sedimentology of this section was logged at a

115   scale of 1 m = 2 cm and is summarized in Figure 3.

116   A 500 m core through gently dipping Ballagan Formation strata was obtained from a

117   borehole at Norham West Mains Farm (Norham borehole), about 8 km SW of Berwick-upon-

118   Tweed (NT 91589 48135, BGS borehole ID: NT94NW20). The base of the Ballagan

119   Formation was not reached and the only direct correlation between the borehole and coastal

120   section is near the top of the succession (Fig. 3). The cores were transferred to the UK's

121   National Geological Repository at the British Geological Survey in Keyworth, Nottingham,

122   where they were cut in half lengthways and photographed. One half of the core is an archive

123   reference and the other half was sampled for this study. The core was logged at a scale of 1 m

124   = 8 cm (Fig. 3).

125   The third section is the 46 m thick succession near to the base of the Ballagan

126   Formation exposed in a river cliff at Crumble Edge near Duns (NT 79276 56412). This

127   section was logged at a scale of 1 m = 2 cm (Fig. 3).

128 *3.2. Field techniques*

129   Palaeosols were identified in the sections, initially by the presence of root traces or

130   pedogenic changes to the sediment such as the development of palaeosol horizons (Retallack,

131   1993, 1997). The palaeosols were numbered sequentially, and prefixed by a three-letter

132   locality code (i.e., NOR = Norham and BUR = Burnmouth). Profile descriptions include

133   horizonation, horizon thickness, nature of the contact between horizons, Munsell colour,

134   reaction to acid, carbonate features using the classification scheme of Machette (1985), trace

135   fossils present and gleys (Appendix A). Standard-sized, polished thin sections (20 μm thick)

136   were made of selected samples of the palaeosol, including desiccation surfaces and carbonate

137   nodules. Thin sections were examined using an Olympus petrographic microscope.

138   The palaeosols were divided into 'pedotypes'; where palaeosols are mapped based on

139   a reference profile for definition (Bown and Kraus, 1987; Retallack, 1994). This approach

140   focuses on the local environmental conditions that formed the palaeosol, rather than focusing

141   on the lateral extent of a particular palaeosol as in the pedofacies approach proposed by

142   Kraus (1999). The pedotype approach is more applicable in this study because it is not

143   possible to trace a single palaeosol between the core and sections.

144

145   *3.3. Analytical techniques*

146   Palaeosols were sampled at 10 cm vertical intervals. This sampling interval was

147   chosen because it is typical for detailed elemental redistribution studies in soils (Adams et al.,

148   2011; Driese, 2004). Thirty-five samples from six palaeosols, representing the best preserved

149   examples of the palaeosols described below, were analyzed for their major element

150   composition using X-ray fluorescence spectrometry (XRFS). The samples were milled to a

151   homogeneous fine powder (<32 μm), dried overnight at 105°C and pre-ignited at 1050°C

152   before fusion using a pre-fused mixture of lithium tetraborate and lithium metaborate (66/34

153   percent ratio). The fusion melt was cast into a 40 mm diameter bead which was analysed

154   using a PANalytical Axios sequential, fully automatic, wavelength-dispersive X-ray

155   fluorescence spectrometer, fitted with a 60 kV generator and 4 kW rhodium (Super Sharp)

156   end-window X-ray tube. The PANalytical calibration algorithm was used to fit calibration

157   curves and inter-element effects were corrected by fundamental parameter coefficients. The

158   analytical method is accredited to ISO 17025 and calibrations have been validated by analysis

159   of a wide range of reference materials. Data were reported in weight percent and have been

160   converted to molar concentrations from which the characteristic parameter ratios hydrolysis,

161   leaching, provenance (acidification), salinization, and chemical affinity are calculated (for

162   results see Appendix B). Palaeosol weathering ratios were calculated using CIA-K (Eq. 1, of

163   Sheldon et al., 2002) and CALMAG weathering ratios (Eq. 2, of Sheldon et al., 2002):

$$CIA - K = [Al_2O_3/(AL_2O_3 + CaO + Na_2O)] \times 100$$

164   (1)

$$CALMAG = [Al_2O_3/(AL_2O_3 + CaO + MgO)] \times 100$$

165   (2)

166   The clay mineralogy of 78 samples from 13 palaeosols selected to represent each of

167   the pedotypes was analysed using X-ray diffraction (XRD) techniques. Samples were

168   included from the sedimentary unit above the soil where this appears unaltered by

169   pedogenesis, to provide a reference for the background lithology of the overbank deposits

170   prior to pedogenesis. Less than 2 μm fractions were isolated, orientated mounts prepared and

171   analyzed using a PANalytical X'Pert Pro series diffractometer equipped with a cobalt-target

172   tube, X'Celerator detector and operated at 45 kV and 40 mA. Mounts were scanned from 2 -

173   40°2θ at 1.02°2θ/minute after air-drying, ethylene glycol-solvation and heating at 550°C for 2

174   hours. Clay mineral species were then identified and quantified from their characteristic peak

175   positions, their reaction to the diagnostic testing program and modelling of the <2 μm glycol-

176   solvated XRD profiles using Newmod II™ (Reynolds and Reynolds, 2013) software. Full

177   details of the methodology employed are given in Harrington et al. (2004) (for results see

178   Appendix B).

179   For stable isotope analysis, the calcite was hand sampled with a microdrill. The

180   calcite was ground finer in agate and the equivalent of 10 mg of carbonate was reacted with

181   anhydrous phosphoric acid *in vacuo* overnight at a constant 25°C. The CO_2 liberated was

182   separated from water vapour under vacuum and collected for analysis. Measurements were

183   made on a VG Optima mass spectrometer. Overall analytical reproducibility for these

184   samples is normally better than 0.2‰ for $\delta^{13}C$ and $\delta^{18}O$ (2σ). Isotope values ($\delta^{13}C$, $\delta^{18}O$) are

185   reported as per mil (‰) deviations of the isotopic ratios ($^{13}C/^{12}C$, $^{18}O/^{16}O$), calculated to the

186   VPDB scale using a within-run laboratory standard calibrated against NBS standards (for

187   results see Appendix B).

188   **4. Results**

189

190   *4.1. Palaeosol facies*

191   In the section at Burnmouth 64 palaeosols were identified, compared with 216 in the

192   Norham core (Fig. 3) even though these two sections are of similar thickness and thought to

193   represent approximately the same period of time. The range of palaeosol thickness is similar:

194   0.02 - 1.85 m at Burnmouth and 0.02 - 1.58 m in the Norham Borehole (Appendix A). The

195   thinnest palaeosols are identified by the presence of thin root mats (Fig. 4A) whereas the

196   thicker palaeosols show many more pedogenic features (e.g. Fig. 4D). Comparing the two

197   successions, there are similar numbers of palaeosols thicker than 0.60 m, but there are

198   significantly fewer palaeosols thinner than 0.60 m recorded at Burnmouth compared with the

199   Norham Borehole (Fig. 3). It seems likely that the number of palaeosols identified at

200   Burnmouth is an underestimate, probably because much of the exposure of the fine-grained

201 rocks is degraded by weathering and it is hard to see fine detail such as root traces. The

202 number of palaeosols recorded in the borehole is probably a truer representation of the

203 frequency of palaeosols developed in the Ballagan Formation. The short section of the

204 Ballagan Formation from near its base at Crumble Edge contains 18 palaeosols with a

205 thickness range of 0.05 - 0.40 m.

206   The palaeosols identified in these sections have been classified into four pedotypes

207 based on the features found such as pedogenic slickensides, nature of the gleys and

208 development of B horizons. These are labelled Pe, Pi, Pg, Pv (Table 1, Fig. 4).

209 *4.2. Pedotype Pe*

210   This pedotype is present in beds of sandstone and siltstone where roots occur at the

211 top of the unit (A horizon). No other subsurface pedogenesis is evident, as the rock shows

212 primary sedimentary lamination (such as cross-bedding) and is thus classified as a C horizon

213 (Fig. 4A). Individual examples of this pedotype are 2 - 35 cm thick, although stacked

214 packages up to 54 cm thick occur where repeated flooding events have formed a compound

215 profile (cf. Kraus, 1999). In stacked sequences, root traces cover 5 - 25 % of the bed which

216 can be overlain by more developed palaeosols. The root traces vary from single tapering

217 structures to branching and interlocking mats (Fig. 5B). Most of the root traces are similar to

218 small rootlets and tap roots (cf. Retallack, 1988) or Type C rooting structures described by

219 Pfefferkorn and Fuch (1991).

220 *4.3. Pedotype Pi*

221   This pedotype shows some development of a reddened pedogenic B horizon where

222 sedimentary lamination has been destroyed by soil formation processes (Fig. 4B). The

223 thickness is 4 - 63 cm. At the top of approximately 50% of this pedotype is a 1 - 30 cm thick

224 gleyed horizon (Eg) which is greenish grey to greyish green (5GY 5/1 to 5G 4/2) in colour.

9

225   This horizon is internally homogenous, although it is commonly disrupted by carbonized

226   roots and polygonal cracks. In the rest of the paleosols the E horizon is not seen. The B

227   horizon is 3 - 63 cm thick and light reddish brown to red (2.5YR 6/3 to 10R 5/6). This

228   horizon lacks sedimentary lamination, shows an increase in clay content and contains drab

229   root halos. This pedotype also has sporadic yellow (2.5Y 8/6) mottles and iron oxide spots 1 -

230   2 mm diameter (Fig. 4B photograph). Some of this pedotype passes down into laminated

231   units, 5 - 40 cm thick, with a small amount of pedogenic alteration (C horizon).

232   Root traces in this pedotype are preserved as carbon films in the gleyed horizons or

233   either drab root halos or filamentous root traces below. The most common are tapering tubes,

234   but root mats, lateral roots and sinuous filaments were also observed.

235   *4.4. Pedotype Pg*

236   Pedotype Pg is defined by the presence of a gleyed (10G 8/1 - 10B 8/1) B horizon and

237   the absence of reddening in any horizon (Fig. 4C). The pedotype is 2 - 80 cm thick. The

238   uppermost horizon, 5 - 15 cm thick, in 11% of examples of this pedotype is black in colour

239   (N1) and has a total organic carbon content (TOC) of 0.5 - 4.7 % compared with the average

240   of c. 0.1% for other siltstones in the succession. This horizon is interpreted to be an O

241   horizon. The other examples of Pedotype Pg have a 2 - 45 cm thick, light greenish grey (5BG

242   7/1 - 10BG 8/1) horizon at the top.

243   The gleyed B horizon horizon is 10 - 73 cm thick and commonly contains yellow

244   (2.5Y 7/6) mottles and ferro-siderite nodules 0.2 - 1 cm in diameter. Roots are less common

245   than in upper horizons, but where found are preserved as carbonized films which tend to be

246   vertical with sporadic branches. This pedotype becomes less massive below the gleyed

247   horizon and starts to show primary sedimentary lamination, though root traces are still

248   present. This is a C horizon, 3 - 23 cm thick and rests on pedogenically unaltered sedimentary

249   rock.

250   The top of pedotype Pg with an O horizon is brecciated (Fig. 6A) in zones up to 25

251   cm, but more commonly 2 - 5 cm, thick. Cracks initiated deep in the profile broaden upwards

252   and grade into the area of brecciation. At first the blocks are 2 - 3 cm across and have a jig-

253   saw fit. The blocks become increasingly smaller upwards and their edges more irregular as

254   the proportion of the overlying sediment between the blocks increases. There is no evidence

255   of rounding or internal fracturing of the blocks. This may be alteration of the original ped

256   structure of the soil.

257   *4.5. Pedotype Pv*

258   Examples of this pedotype are 0.32 - 1.85 m thick. They are defined by the red colour

259   throughout the Bt horizon and by the presence of deeply penetrating vertic cracks (Table 1,

260   Fig. 4D). Over 60% of this pedotype have a gleyed top, 10 - 30 cm thick which is dark

261   greenish grey to pale green (5G 4/1 to 5G 6.2) in colour. This layer has filamentous root

262   traces which are preserved as carbon films. The main horizon below is 35 - 123 cm thick and

263   dusky red to red (2.5YR 3/2 to 10R 5/6). This layer contains minor pale green (5G 4/1)

264   mottles and root traces preserved as drab root halos. In the thicker units these have an affinity

265   with tap rooting structures (cf. Type H, Pfefferkorn and Fuch, 1991). Some of the better

266   developed examples of this pedotype contain bands up to 15 cm thick of pedogenic carbonate

267   nodules at depths of more than 1 m. The nodules are 0.5 - 2 cm in diameter and are of stage II

268   calcrete development (cf. Machette, 1985). The carbonate nodules are indicative of a Bk

269   horizon; where carbonate is absent this is the Bt horizon. Low-angle pedogenic slickensides

270   may also be present in the Bt horizon outcrop but due to weathering cannot be confirmed.

271   Below this the pedotype passes down into reddened, laminated mudstone (C horizon).

11

272   The Pv pedotype is commonly overlain by beds of flood-generated sandy siltstone

273   (Bennett et al., 2016). These beds mostly have a gley colour and also fill cracks in the top of

274   the pedotype (Fig. 6B). The downward-tapering cracks are up to 38 cm long and 2 cm wide at

275   the top. Most cracks are near vertical although there are horizontal and oblique examples,

276   some of which radiate from the larger cracks (Fig. 6B). The margins of the cracks are

277   irregular with finer cracks penetrating into the adjacent pedotype. Also, angular clasts of

278   siltstone up to 1 mm appear broken off from the crack margin and have a jig-saw fit with the

279   unfractured crack margin. There is commonly a zone of pale green gley (5G 4/1) up to 1 cm

280   from the cracks (Fig. 6B). There are also rare examples of cracks filled with fine-grained

281   sandstone.

282   *4.6. Root traces*

283   The diverse root traces found in the palaeosols of the Ballagan Formation range from

284   1 to 80 cm long. The simplest of these traces occurs in very fine-grained sandstone and

285   siltstone beds less than 10 cm thick. They taper downward and have sinuous sides (Fig. 5A).

286   These features are most similar to fibrous root systems (Retallack, 1988) or Type D rooting

287   structures described by Pfefferkorn and Fuch (1991) and may be plug roots, but are often

288   hard to distinguish from *Planolites*. In pedotype Pe rootmats are common (Fig. 5B). These

289   root traces typically penetrate less than 1 cm into the sand unit and are preserved as carbon

290   infills. Rooting associated with the more developed Pi pedotype commonly exhibits

291   downward penetrating single fibres with sporadic branches 0.1 - 0.5 cm diameter. Individual

292   roots penetrate 5 - 15 cm into the palaeosol. In the reddened horizons they are preserved as

293   drab root halos (Fig. 5E). These have most affinity with simple fibrous vertical roots with

294   occasional branches (Type D rooting structures described by Pfefferkorn and Fuch, 1991).

295   The root traces of pedotype Pg are preserved as carbon films (Fig. 5C). This type of

296   root is mostly vertical, 2 - 4 cm long, with sporadic branches and concentrated in the top 20 -

297   30 cm of the palaeosol. There are some horizontal root traces at the top of the pedotype and

298   these appear to form root mats. Roots are only sporadically preserved lower down in the

299   profile. These roots are similar to tabular root systems with sporadic lateral roots (Retallack

300   1988; Type G roots of Pfefferkorn and Fuch, 1991).

301   A lycopsid root is preserved in one example of pedotype Pi at Crumble Edge (Fig.

302   5D). The root is 38 cm long and 8 cm wide, tapers to a point and has lines of pits along its

303   surface. Sediment is disrupted around the root which appears to be in situ. The root is filled

304   with sand which probably infilled once the woody material within the root decayed, a

305   mechanism suggested by Gastaldo (1986).

306   In pedotypes Pi and Pv which have a developed Bt or Bk horizon roots penetrate to

307   depths of up to 80 cm (Fig. 5F, G). The roots are preserved as drab root halos and comprise a

308   linear trace with sporadic bifurcation. Some of these root traces appear to have tapering tips

309   and may be similar to adventitious roots (Retallack, 1988). A second set of horizontal, tubular

310   root traces 0.5 - 2 cm diameter occurs in the thickest of pedotype Pv at depths of 100 cm (Fig.

311   5F). It is unclear whether these are connected to the vertical drab root halos above or are a

312   separate rooting structure.

313   *4.7. Polygonal cracks*

314   In addition to the vertic cracks of pedotype Pv and the fractured and brecciated

315   pedotype Pg, minor polygonal cracks are found at the top of pedotypes Pi, Pg and Pv. The

316   cracks are 5 - 8 cm deep and originate from the top of the palaeosol. They mostly taper

317   downwards and have irregular, sharp edges. When viewed on a bedding plane these cracks

318   form polygons (Fig. 6C). Silt-grade sediment containing a large percentage of angular, 0.2 -

13

319   0.5 mm organic fragments along with muscovite grains and subangular quartz fragments fills

320   the cracks. In most cases this sediment is flood-generated sandy siltstone and identical to the

321   overlying bed (see Bennett et al., 2016). Small (0.2 mm), angular clasts of the palaeosol may

322   be present in the sediment filling the crack (Fig. 6D). The polygonal cracks are identified as

323   prismatic peds (Retallack, 1988).

324   *4.8. Carbonate morphology and isotope composition*

325   Three palaeosols of pedotype Pi and Pv in the section at Burnmouth contain carbonate

326   nodules 2 - 15 cm in diameter, and are of stage II calcrete development (cf. Machette, 1985).

327   In the Norham Borehole eighteen palaeosols contain carbonate nodules 0.2 - 3 cm in

328   diameter. Some nodules occur in discrete (Bk) horizons, but most others are found

329   throughout the palaeosol.

330   The boundary of the nodule with the surrounding sediment is commonly diffuse (Fig.

331   7A), although in some there is an indication of mineral alignment around the carbonate

332   nodule, suggesting they may have been affected by vertic movements in the soils (Fig. 7B).

333   The carbonate nodules are mostly micritic calcite (crystal size 5 - 18 μm), with sparry calcitic

334   centres, possibly filling a void (Fig. 7A). There are also examples of carbonate concretions

335   forming around and within, root traces. These comprise a rim of micritic calcite which forms

336   around the root trace and commonly a centre of larger (30 μm) calcite crystals filling a central

337   void in the root (Fig. 7C). A further type of carbonate nodule, again with diffuse margins

338   (Fig. 7B), comprises an aggregate of 20-μm rhomb-shaped dolomite crystals surrounded by

339   larger crystals of calcite. All of these carbonate accumulations contain floating grains of sub-

340   rounded quartz.

341   Only two palaeosols (BUR 59 and NOR 37) contain nodules that were formed of

342   calcite rather than dolomite. The calcitic parts of these carbonates were handpicked and

14

343   crushed to a powder. The micritic calcite parts of the nodule have isotope values within the

344   range of $\delta^{13}C$ of -5.65 ‰ to -6.85‰ and $\delta^{18}O$ -6.85 ‰ to -7.14 ‰ (Fig. 7E). The late vein

345   fills and the coarser, sparry core of nodules have a similar range of isotope values for $\delta^{13}C$ of

346   -5.65‰ to -6.56 ‰ and $\delta^{18}O$ of -6.83 ‰ to -11.39 ‰ (Fig. 7E, Appendix B).

347   *4.9. Clay mineralogy*

348   In general terms, all palaeosols analysed show a similar clay mineral assemblage and

349   are predominantly composed of illite/smectite (I/S) and illite with minor amounts of chlorite

350   ± traces of kaolinite. NEWMOD-modelling of the XRD traces enabled the precise speciation

351   of the I/S present (from an evolved, 92 % illite, *R*3-ordered species to a less evolved, more

352   smectitic 80 % illite, *R*1-ordered species) and enabled traces of kaolinite to be distinguished

353   in the presence of chlorite (Fig. 8, Appendix B). The <2 μm analyses also reveal the presence

354   of non-clay minerals, principally quartz, plagioclase feldspar, hematite, goethite and sporadic

355   calcite, dolomite, jarosite and siderite.

356

357   *4.10. Major element geochemistry*

358   All of the palaeosols show a broad increase in the Al/Si ratio with depth, reflecting the

359   growth of clay minerals during pedogenesis (Fig. 9, Appendix B). This is most evident in the

360   pedotype Pv, before passing into the more silica-rich C horizon. The thicker palaeosols at the

361   top of the section (Fig. 9: NOR5, NOR6) also show an increase in Al/Si ratio in the top 40

362   cm. This may be due to the inclusion of flood-generated sandy siltstone filling many of the

363   vertic cracks present in the top 40 cm of these profiles. The increase in clay content with the

364   more developed palaeosols indicates the development of Bt horizons of pedotypes Pv and Pi.

365   However, these have relatively elevated Al/Si ratio values compared with the average for

366   palaeosols in general (cf. Retallack, 1997).

367   (Ca + Mg)/Al is a proxy for the amount of carbonate in the soils (Retallack, 1997).

368   From this, the Ballagan Formation palaeosols have very low carbonate values, possibly

369   because of their relative immaturity, although there is an increase in the amount of Ca + Mg

370   in one of the thicker palaeosols of pedotype Pv, reflecting the presence of carbonate

371   accumulation in that palaeosol (Fig. 9: NOR5). Fe/Al varies little between the palaeosols

372   (Fig. 9), but the redox state of the iron was not determined in this study.

373   Salinization ((Na+K)/Al) tracks the amount of alkali elements accumulated in the soil

374   (Sheldon and Tabor, 2009). This separates the higher ratios of the more waterlogged

375   pedotypes Pg and Pi, from the drier pedotype Pv (Fig. 9).

376   The Ti/Al ratio is used to assess potential changes in provenance in the parent

377   material (Myers et al., 2014; Sheldon and Tabor, 2009). The molar ratios are 0.02 - 0.04 with

378   a median value of 0.03. There is no variation with stratigraphic depth, suggesting there has

379   been no major change in provenance of the source material throughout the Ballagan

380   Formation.

381

382   **5. Discussion**

383   *5.1. Pedotype interpretation*

384   The simplified interpretation of USDA Soil Taxonomy can be used to relate the

385   pedotypes found in the Ballagan Formation to modern soil types (Retallack, 1993, 1994; Soil

386   Survey Staff, 1999). There is debate about how far a classification scheme created for modern

387   soils can be applied to palaeosols and other classification schemes have been suggested

388   (Mack et al., 1993; Mack and James, 1994; Retallack, 1993, 1994; Krasilnikov and Calderón,

389   2006; Nettleton et al., 1998, 2000). However, comparison with modern soil types is useful to

390   inform interpretations of the environment in which the palaeosols formed.

391   Pedotype Pe shows an absence of subsurface pedogenic horizons which indicates that

392   the palaeosols formed quickly before sediment buried them. This is characteristic of the more

393   active areas of the floodplain of many fluvial systems today, for example on river sand bars

394   which have been stable long enough for plants to become established. Based on the shallow

395   rooting depths and absence of subsurface pedogenic horizons, this pedotype is most likely to

396   be an Entisol, as suggested by Retallack (1993, 1994) (Table 1). Using the classification of

397   Mack et al. (1993) these are Protosols (Table 1).

398   Pedotype Pi shows greater development of subsurface pedogenic horizons than

399   pedotype Pe. The root networks in the Bt horizons are poorly preserved, but appear

400   filamentous and branching. Pedogenic processes have removed any primary depositional

401   structures in the horizon which is distinctly reddened and interpreted to be a cambic horizon

402   as defined by Retallack (1994).

403   The presence of a gleyed surface horizon (Eg) and a cambic horizon (Bt) below are

404   characteristic of Inceptisols as suggested by Retallack (1993, 1994) (Table 1). This suggests

405   that they formed further away from the active river system than the Entisols; episodic

406   flooding deposited new sediment on top of the palaeosols thus preventing further

407   development. Using the classification of Mack et al. (1993) these would also be classified as

408   Protosols.

409   The gleyed colour of the Pedotype Pg, along with root traces preserved as carbon

410   films and the occurrence of ferro-siderite nodules all suggest permanent water logging

411   (Retallack, 1994; Kraus and Hasiotis, 2006). The TOC content of the O horizon is too low

412   for these palaeosols to be classified as Histosols and they are therefore more likely to be

413   gleyed Inceptisols following Retallack (1993, 1994) or Gleysols, using the classification of

414   Mack et al. (1993).

17

415   Palaeosols with similar features to pedotype Pg have been described from Devonian

416   sedimentary rocks in New York, USA by Retallack and Huang (2011). The lack of a peaty

417   horizon in those palaeosols led to their classification as gleyed Inceptisols. However, it is

418   evident that some of the palaeosols seen in the Ballagan Formation have an organic horizon

419   preserved whereas others do not; yet they share most other features. The absence of an O

420   horizon may be because it has been eroded, or did not have time to form.

421   Brecciation of the top of some of these palaeosols is unique to pedotype Pg and most

422   likely formed in situ (Fig. 6A). The brecciation may be caused by disaggregation of the peds

423   on the top of the palaeosol, but this occurs only in permanently water-logged palaeosols, and

424   soils formed under water-logged swampy conditions typically lack soil ped structure

425   (Retallack, 1988). However, this feature resembles soil crusts and vesicular surface horizons

426   seen in modern saline-sodic wetland soils (Joeckel and Clement, 2005). Unlike desiccation or

427   vertic cracks, these form in permanently water-logged soils and are confined to the very top

428   of the soil. They form on a daily to seasonal time scale by repeated cycles of salt

429   development, microbial activity and microrelief genesis, controlled by regular wetting and

430   drying cycles interacting with ponded surface- and ground-waters (Joeckel and Clement,

431   2005). The palaeosols were dynamic and over time created surface soil textures which are

432   extensively slaked or flaked.

433   Compared with other pedotypes from the Ballagan Formation, the Pv palaeosols are

434   thicker and better developed. Any original, internal sedimentary structure in the siltstone has

435   been overprinted completely by pedogenic processes. They are characterised by deep cracks,

436   putative pedogenic slickensides, thick clayey horizon (Bt) and sporadic carbonate nodules

437   indicating that these palaeosols are Vertisols, using either the USDA Soil Taxonomy or

438   classification of Mack et al. (1993). They represent periods of relative stability on the

439   floodplain where areas remained above the water table long enough for the thick profiles to

440   develop (cf. Kraus, 1999).

441   The deep penetrating cracks (Fig. 6B) are similar to those reported from modern

442   floodplain soils by Rust and Nanson (1989) and to the vertical cracks identified by Caudill et

443   al. (1996) in late Mississippian palaeosols from Tennessee. The latter are associated with

444   gilgai micro-topography, with the cracks forming at the centre of vertic 'pseudo-anticlines'

445   on micro-highs. However, as only single deep penetrating cracks have been identified in

446   individual palaeosols in the cores from the Ballagan Formation, it is impossible to measure

447   the distance between putative micro-highs and micro-lows. The depth of cracking and the

448   poorer preservation potential of micro-highs (Driese et al., 2000) may indicate that these

449   palaeosols are micro-lows, probably formed in low topographic areas. The gleyed colour

450   associated with these cracks is probably a surface water gley caused by rapidly deposited

451   flood waters which deposited the flood-generated sandy siltstone in the cracks (Bennett et al.,

452   2016).

453   The carbonate nodules found in palaeosols of this pedotype have two potential

454   origins: they may indicate that the palaeosol dried out during periods of high evaporation

455   (Breecker et al., 2009), or they may have formed during groundwater movement. A few of

456   the nodules examined show evidence of neomorphic replacement. According to Wright and

457   Tucker (1991) this is common within soil carbonate even when the soil is still part of the

458   active vadose zone. However, it can also be a later diagenetic fabric in which the crystal

459   contacts are characteristically concavo-convex (Fig. 7C), and enclose smaller patches of

460   microcrystalline dolomite (Quast et al., 2006). Most of the carbonate found in the palaeosols

461   in the Ballagan Formation exhibits alpha textures, although the calcified root traces (Fig. 7A -

462   D) could be attributed to beta textures as defined by Alonso-Zarza and Wright (2010) and

463   Wright and Tucker (1991). The presence of neomorphic replacement with calcite suggests a

464   degree of alteration after the nodules formed.

465   The isotopic results from the calcitic nodules show more negative δ^{13}C and δ^{18}O

466   values than ferroan dolostone beds found in the same sections (Fig. 7E). This is a similar

467   pattern to that seen between paludal dolomites and calcretes from the Late Mississippian of

468   Kentucky, USA (Barnett et al., 2012). In that locality it was suggested that the relative offsets

469   were due to the calcretes forming from meteoric water while the paludal dolomites formed in

470   brackish water conditions. A similar relationship has beens seen elsewhere in the Ballagan

471   Formation in central Scotland (Williams et al., 2005). However, the isotopic results from the

472   calcitic nodules in this study, overlap with the values from late vein fills and coarser,

473   recrystallized core of nodule (Section 4.8). Turner (1991) and has recorded similar isotope

474   values from phreatic calcite cement in sandstones in study of carbonates from the Ballagan

475   Formation (Fig. 7E) suggesting palaeosol carbonate has been diagenetically altered.

476   *5.2. Clay minerals*

477   Pedogenesis tends to alter detrital clays to smectite (Sheldon and Tabor, 2009).

478   Though smectite was not detected in any of the samples, some clay assemblages are

479   composed of more than 55 % I/S and, given the burial depth, it seems likely that this was

480   derived from the original pedogenic smectite. I/S increases proportionally with depth in the

481   palaeosols, especially in the Vertisols (Fig. 8), suggesting that original pedogenic trends are

482   retained.

483   Illite and chlorite are generally considered to have been inherited from parent rock or

484   other material (Wilson, 1999). However, Joeckel and Clement (2005) showed that repeated

485   wetting and drying cycles caused illitization in modern saline-sodic wetland soils, resulting in

486   illite dominating the basin surface of the soil, with smectite becoming dominant at depth. In

20

487   the gleyed Inceptisols with brecciated tops, the uppermost 10 cm are dominated by illite (and

488   more illitic I/S) and the lower parts are dominated by more smectitic I/S suggesting that

489   illitization may have occurred here in the Ballagan Formation palaeosols (Fig. 8).

490   Alternatively, this may be because the floodplain material on which the palaeosols were

491   forming was illite-rich.

492   Kaolinite forms a minor-trace component of the clay assemblages present in all

493   palaeosols, but is more prevalent in the Inceptisols and Entisols. Kaolinite forms under acid

494   soil conditions and is often cited as a proxy for more arid palaeoclimatic conditions (Sheldon

495   and Tabor, 2009).

496   Hematite and/or goethite are also present in all of the palaeosols. In the Vertisols only

497   hematite is present in the Bt horizon, whereas hematite and goethite are present in the Eg

498   horizon. Inceptisols and gleyed Inceptisols, by contrast, contain both hematite and goethite

499   throughout the palaeosol. Goethite is known to form in permanently water-logged

500   environments (Sheldon and Tabor, 2009; Tabor et al., 2004) and this supports the link

501   between the gleyed horizons in the palaeosols and water logging.

502   I/S species are transitory phases and do not typically persist in soil profiles. In

503   addition, there is little published evidence for long-range ordered (R3) I/S or precursor

504   randomly interstratified (R0) I/S forming stable phases in soils (Wilson, 1999). The presence

505   of I/S and absence of discrete smectite in the Ballagan Formation palaeosols therefore

506   suggests that the detected clay mineral assemblages have developed through burial diagenesis

507   of original pedogenic smectite.

508   From the range of I/S compositions detected, the maximum burial depth of between 3

509   – 6 km is suggested, assuming a 30 °C/km geothermal gradient (Merriman and Kemp, 1996).

510   A vitrinite reflectance value (Rv) of 0.54 was determined on coal-like samples from the

21

511 Norham borehole (D. Carpenter, pers. comm. 2015). Comparing this value with the Rv

512 gradient for Fife obtained by Marshall et al. (1994), predicts a burial depth of about 2.5 km,

513 in broad agreement with that predicted by the least evolved I/S compositions. The deeper

514 burial depths suggested by the more evolved I/S most likely reflect more advanced diagenetic

515 progression hosted by slightly different palaeosol compositions.

516 *5.3. Palaeosol floodplain associations*

517 The diversity of palaeosols in the Ballagan Formation indicates a dynamic floodplain.

518 The most common palaeosol in the three sections examined is Inceptisol (Pi), with 49 % at

519 Burnmouth, 42 % at Norham (Fig. 10) and 67 % at Crumble Edge. This palaeosol represents

520 a relatively short period of soil development, long enough for clay-rich sub-horizons to

521 develop, but not long enough to develop any other pedogenic structures; they are thought to

522 take 100s to 1000s of years to form (Retallack, 1998; Kraus, 1999). They may have formed

523 near to fluvial channels.

524 The next most common palaeosol in the Norham core is gleyed Inceptisol (Pg) (27 %:

525 Fig. 10), but its low frequency in the two field sections probably results from the difficulty of

526 identification in weathered 'shale' sections. The gleyed character of these palaeosols,

527 preservation of roots as carbon, and brecciation, suggest that these soils formed in wetlands,

528 although none is capped by coal. The root traces in these palaeosols are vertical with sporadic

529 lateral branches (Fig. 5C), reminiscent of fibrous rooting systems (Pfefferkorn and Fuch,

530 1991; Retallack, 1988). This suggests that they represent marshland, defined as wetland

531 dominated by herbaceous or shrub-like vegetation on a mineral (non-peat) substrate (Greb et

532 al., 2006). The presence of a thin O horizon in 11 % of the gleyed Inceptisols implies that

533 small mires developed locally.

534   Vertisols represent only 9 % of the palaeosols identified in the Norham core,

535   suggesting that they probably developed above the water table on relatively small and

536   isolated areas on the floodplain (Fig. 10). At 23 % Vertisols are considered to be

537   proportionally over-represented in the Burnmouth section, probably because they are easier to

538   identify than the other, generally thinner palaeosols. However, approximately similar

539   numbers (19 and 15 respectively) were recorded.

540   Although no direct correlation between root length and the size of the plant above

541   ground has been found (Raven and Edwards, 2001), rooting depths of 80 - 100 cm seen here

542   have been considered by Algeo and Scheckler (1998) to be associated with arborescent plants

543   from the Famennian onward. We did not find any tree stumps from the Vertisols. However,

544   examples at the base of some of the beds overlying Inceptisols (Fig. 5H), are similar to those

545   reported from the Tournaisian Horton Group in eastern Canada by Rygel et al. (2006). The

546   trunks in the Horton Group have diameters of 10 - 110 cm, whereas those found at

547   Burnmouth in the gleyed Inceptisols range from 6 to 14 cm. Using the relationship of tree

548   width to its height (Eq. 3) proposed by Niklas (1994); where H is tree height in meters and B

549   is the diameter of the trunk in meters (R^2 = 0.95 and S.E. = ±0.9 m):

$$H = 21.9B^{0.889}$$

550   (3)

551   The trees in the gleyed Inceptisols at Burnmouth were no taller than 3.8 m. It is

552   known from other Ballagan Formation sections near Foulden, just 6 km SSW of Burnmouth,

553   that the gleyed Inceptisols were dominated by small shrubby ferns such as *Lyrasperma*

554   *scotica* (Retallack and Dilcher, 1988). At this locality tall forest trees have also been found,

555   such as *Stamnostoma huttonense,* which have trunk diameters of 1.4 m and are thought to

556   have been up to 25 m tall. These are interpreted by Retallack and Dilcher (1988) to have

23

557 grown on the better drained palaeosols. This suggests that the forests were restricted to those

558 areas where thick, better drained palaeosols were present.

559 Vertisols are only present in the uppermost 200 - 300 m of both the section at

560 Burnmouth and in the Norham core (Fig. 10). This could indicate that there is increasing

561 aridity later in the Tournaisian. However, this is not corroborated by any of the other

562 palaeosols, such as the gleyed Inceptisols which are generally constant through the section.

563 Alternatively, the abrupt appearance of Vertisols may be due to palaeosol progradation rather

564 than climatic change.

565 In the Norham core 29 % of the palaeosols preserve polygonal or vertic cracks.

566 Although this result could not be replicated at Burnmouth due to poor exposure of many of

567 the palaeosols tops, this suggests that the floodplain was frequently exposed to periods of

568 evaporation and desiccation. High evaporation rates are also implied by the presence of thin

569 evaporite beds in the Norham core and in other sections by sporadic siltstone pseudomorphs

570 after halite (Andrews et al., 1991; Turner, 1991; Williams et al., 2005).

571 More than half of the Inceptisols, gleyed Inceptisols and Vertisols have a gleyed

572 surface horizon (Eg), commonly overlying a reddened Bt or Bk horizon. The presence of drab

573 root halos, together with the gley horizon, but absence of siderite nodules implies that the

574 soils may have been flooded by surface water (Retallack, 1994). Flood-generated sandy

575 siltstone beds overlying many of these palaeosols have been interpreted to result from low-

576 energy flooding events, supporting this hypothesis (Bennett et al., 2016). The preservation of

577 roots as carbon films, rather than as drab root halos, in the uppermost part of the palaeosol

578 and within the flood-generated sandy siltstones, indicates that the flood waters were poorly

579 oxygenated or that deposition was rapid. Retallack et al. (1985) and Retallack and Huang

580 (2011) have described similar palaeosols from upper Devonian strata in New York State, as

581   have Caudill et al. (1996) and Bashforth et al. (2014) from the Carboniferous of New

582   Brunswick, Canada. They are interpreted to be surface water gleys where stagnant water has

583   filled root channels (Kraus and Hasiotis, 2006).

584   The picture that emerges is of a floodplain where bodies of standing water are

585   juxtaposed with areas of developing soils (Fig. 11). Pedogenesis was regularly interrupted by

586   low-energy flooding events (Bennett et al., 2016). By contrast, the thick Vertisols represent

587   parts of the floodplain that were less affected by flooding as, based on their thickness and

588   level of development, these soils could have taken thousands of years to develop (cf.

589   Retallack, 1994). Overall, the palaeosols suggest that the Ballagan Formation floodplain was

590   a diverse seasonal wetland (Fig. 12). It is not possible to determine the lateral extent of the

591   different palaeosol types from the core and sections at Burnmouth and Crumble Edge. It is

592   also not possible to trace any particular palaeosol between the sections. However, the

593   occurrence of all the palaeosols throughout both sections suggests that a mosaic of

594   environments co-existed.

595   Andrews et al. (1991) and Stephenson et al. (2002) have suggested that the Ballagan

596   Formation contains evidence of marine incursions which Andrews et al. (1991) envisaged as

597   short-lived events, possibly storm surges. The high frequency of palaeosols throughout the

598   Ballagan Formation (Fig. 10) suggests that at no time was there a prolonged marine flooding

599   event in the Tweed Basin.

600   *5.4. Palaeoprecipitation and seasonality*

601   The CIA-K and CALMAG weathering ratios of palaeosols with a Bw or Bt horizon

602   (Fig. 9) can be used to determine mean annual precipitation (MAP) (Adams et al., 2011;

603   Nordt and Driese, 2010; Sheldon and Tabor, 2009). Many of the palaeosols in this study do

604   not show readily distinguishable chemical enrichments in the lower horizons (Fig. 9)

25

605   precluding the use of such proxies. Typically this is caused by reworking of palaeosol

606   material on the floodplain; however, reworked palaeosol material only makes up a minor

607   component of the parent overbank material (Bennett et al., 2016). To ensure that the

608   palaeosols have undergone significant phyllosilicate weathering Sheldon and Tabor (2009)

609   proposed that only samples with a difference of 5 - 8 units in the CIA-K ratio between the B

610   horizon and the parent material are used in the calculation. Many palaeosols in our study

611   overlie, and are overlain by sediments that have undergone some pedogenesis, and therefore

612   samples without rooting and with primary lamination were selected to act as the closest proxy

613   to the parent material of the palaeosols. As a result of this screening, only palaeosols

614   NOR148, NOR6, and NOR5 were different enough from the parent material to be used to

615   estimate palaeoprecipitation.

616   The screened palaeosols are all Vertisols. Adams et al. (2011) and Nordt and Driese

617   (2010) have claimed that the standard relationship between CIA-K and MAP is not accurate

618   for Vertisols and either a variant of the CIA-K MAP relationship or the CALMAG MAP

619   relationship should be used. The standard CIA-K -MAP relationship gives an estimated

620   average precipitation of 1370 mm per year (max 1501 mm, min 988 mm) through the

621   Ballagan Formation, whereas the CIA-K MAP modified for use with Vertisols gives an

622   estimated average of 1368 mm per year (max 1458 mm, min 1064 mm); a similar estimated

623   average of 1037 mm per year (max 1103 mm, min 811 mm) is obtained from the CALMAG

624   MAP relationship. Stratigraphically, the difference between the average MAP estimates of 74

625   - 112 mm is within experimental error (CIA-K = ±181 mm; CALMAG = ±108 mm) (Nordt

626   and Driese, 2010; Sheldon and Tabor, 2009).

627   The MAP estimates, along with the previously determined palaeolatitude at this time

628   of 4ºS of the equator (Scotese and McKerrow, 1990), enable us to conclude that the northern

629   UK lay within the tropical climate regime (Peel et al., 2007). A monsoonal climate has been

630   proposed for the early Carboniferous of northern Britain based on a study of tree rings by

631   Falcon-Lang (1999) and on Arundian palaeosols in South Wales by Wright et al. (1991). This

632   is supported by plate reconstructions which suggest that the British Isles would be under the

633   Intertropical Convergence Zone, where the highest tropical rainfall occurs. During the

634   southern hemisphere summer it is predicted that a large area of low atmospheric pressure

635   would have formed over Gondwana drawing these rains south and causing a dry season over

636   southern Laurussia (Falcon-Lang, 1999; Wright, 1990).

637   Based on Tournaisian and Visean sections in the south of England, Wright (1990)

638   suggested a semi-arid climate with monsoonal rain. While our study gives palaeoprecipitation

639   values within the modern monsoonal range and provides plentiful evidence of high

640   evaporation rates, we have not confirmed the tendency towards more semi-arid conditions

641   towards the top of the Tournaisian that he demonstrated. This may be related to local

642   floodplain palaeogeography, though in the western Midland Valley of Scotland the Ballagan

643   Formation is overlain conformably by the lower Visean (Chadian) Clyde Sandstone

644   Formation, comprising stacked fluvial sandstone bodies with common calcretes (Andrews

645   and Nabi, 1998; Browne et al., 1999) suggesting a return to semi-arid conditions.

646   The highly variable water table demonstrated by the palaeosols in the Ballagan

647   Formation is illustrated in Figure 11 by the inverse relationship shown between the thickness

648   of palaeosols and that of grey laminated siltstone. In those parts of the sections where

649   palaeosols dominate there is a reduced thickness of grey laminated siltstone. Deposited in a

650   range of settings, from lacustrine to marine, the grey laminated siltstones can be used as a

651   proxy for relatively stable sub-aqueous deposition. This suggests that some parts of the flood

652   plain were under water for long periods and others switched back and forth between

653   palaeosol and bodies of standing water caused by a degree of micro-topography on the

654   floodplain (Fig. 12).

655   Thin evaporite deposits, associated with ferroan dolostones and some with laminated

656   grey siltstones are found throughout the section. Evaporites in seasonal tropical climates have

657   been reported from the Pennsylvanian of New Mexico by Falcon-Lang et al. (2011). In the

658   British Virgin Islands and in wetlands in Ghana that experience a seasonal tropical climate

659   today (similar to that proposed for the Ballagan Formation) salinity in pools, ponds and

660   lagoons varies greatly depending on the degree of connection to the sea (e.g. Jarecki and

661   Walkey, 2006; Gordon et al., 2000). Evaporites such as gypsum crusts form during the dry

662   season when seawater seeps into ponds continuously supplying salts, without introducing

663   sufficient seawater to cause flushing of the deposit (Jarecki and Walkey, 2006).

664   *5.5. Comparison between Famennian and Tournaisian tetrapod sites*

665   Retallack (2011) proposed that the overlap between the intertidal zone and woodlands

666   within brackish mangrove communities is a likely environment in which the transition of

667   tetrapods on to land would occur. By contrast, the Upper Devonian strata of East Greenland,

668   where the largely aquatic tetrapods *Ichthyostega* and *Acanthostega* were found, has been

669   interpreted as an arid, low-sinuosity fluvial and lacustrine system (Astin et al., 2010). The

670   sections there include a 460 m thick, stacked succession of Vertisols. Frasnian to Famennian

671   tetrapods from New South Wales, Australia, are associated with fluvial sandstones and

672   reddened overbank deposits including palaeosols indicative of fairly dry conditions

673   (Campbell and Bell, 1977; Young, 2006). By contrast, Frasnian and Famennian rocks from

674   Red Hill and other localities in Pennsylvania record evidence of lycopsid wetlands and

675   abundant Vertisols and Aridisols with carbonate nodules thought to represent a sub-humid

676   floodplain (Retallack et al., 2009; Cressler et al., 2010; Daeschler and Cressler, 2011). There,

677   tetrapod bones are found in oxbow lake margins. Other tetrapod-bearing sections have shown

678   that in the Famennian tetrapods inhabited environments from brackish lagoons to lakes and

679   woodland-dominated fluvial systems (Retallack, 2011).

28

680   There are few Tournaisian localities worldwide from which palaeosols have been

681   described, and only one of those – Blue Beach, Nova Scotia – has so far yielded tetrapod

682   fossils (Anderson et al., 2015; Falcon-Lang, 2004; Graham, 1981; Moore and Nilsen, 1984;

683   Rygel et al., 2006). The Horton Group in Nova Scotia and the Albert Formation (part of the

684   Horton Group) in New Brunswick contain palaeosols similar to those recorded here in the

685   Ballagan Formation (Falcon-Lang, 2004; Rygel et al., 2006). The palaeosols in the Albert

686   Formation are described as "grey vegetated wetlands, red desiccated mudstone beds are

687   interpreted as well-drained, Entisols and Inceptisols on a vegetated flood basins that formed

688   under a seasonally dry climate as indicated by pedogenic carbonate nodules" (Falcon-Lang,

689   2004). Whereas the palaeosols are similar in both formations, the Albert Formation lacks the

690   cementstone beds that are abundant in the Ballagan Formation. The Horton Group in Nova

691   Scotia contains "nodular and stratified dolomite" and "green rooted mudstones" with

692   abundant tree stump casts (Rygel et al., 2006). However, these sections lack reddened

693   claystones or vertic cracks characteristic of the Ballagan Formation. The broad similarities

694   between the sections in the Horton Group and those in this study suggest that the overall

695   terrestrial palaeoenviroment represented in the Ballagan Formation may have been extensive,

696   but local variations controlled the types of palaeosol that formed.

697   There is evidence that salinity in the Ballagan Formation sediments varied. Evaporite

698   beds and the brecciated gleyed Inceptisols have elevated [Na+K]/Al ratios. Morphologically,

699   the gleyed Inceptisols are similar to the marsh palaeosols reported from the Devonian of New

700   York, USA by Retallack and Huang (2011). However, those soils have [Na+K]/Al ratios

701   identical to the dryland palaeosols in the same section (wetland 0.23 - 0.25; dryland 0.23 -

702   0.28). In our study, the gleyed Inceptisols have [Na+K]/Al ratios of 0.34 - 0.41 compared

703   with 0.25 - 0.37 for the dryland Vertisols. Interpretation of this difference must be cautious

704   because K in particular, can be redistributed during diagenesis and burial (Sheldon and

705 Tabor, 2009). However, the brecciation seen on the top of some of the gleyed Inceptisols,

706 interpreted in to have formed by salt development in the top of the soil, suggests that these

707 palaeosols formed in saline-sodic wetlands (cf. Joeckel and Clement, 2005). Therefore it can

708 be inferred that the vegetation found on these palaeosols must have been halophytic.

709 Furthermore, lycopsid roots are also indicative of very shallow water, and a potentially saline

710 wetland or salt marsh environment (Rygel et al., 2006; Raymond et al., 2010). By contrast,

711 the terrestrial to aquatic vertebrate, arthropod and mollusc fauna present within sandy

712 siltstones that overlie palaeosol beds indicates that floodplain pools and lakes were mostly

713 freshwater to brackish (Bennett et al., 2016).

714 From the Visean onwards tetrapods seem to have preferred swamp woodlands and

715 forest habitats (Retallack, 2011). While the Ballagan Formation does not contain any coal

716 mires or 'swamp' palaeosols (e.g. Sproul pedotype of Retallack et al., 2009 and Retallack,

717 2011), there is a significant increase in the proportion of gleyed palaeosols compared with

718 Famennian sections (e.g. Astin et al., 2010; Retallack et al., 2009; Retallack and Huang,

719 2011). The Tournaisian Ballagan Formation comprises 40 % more grey siltstones than red,

720 compared with the Famennian tetrapod-bearing sections of Red Hills and Pennsylvania

721 (Retallack et al., 2009; Retallack and Huang, 2011; Retallack, 2011) where there are 46 -

722 63 % more red siltstones. Whereas reddened palaeosols cannot be used to indicate aridity

723 (Sheldon, 2005), the comparison suggests that the permanent ground-water table was higher

724 in the Tournaisian sections. This might have been advantageous to tetrapods by providing a

725 diversity of different floodplain water-bodies, such as marshes, pools and lakes, aside from

726 fluvial systems and subaerial habitats. Other animals may have also benefited from the

727 seasonal wetland environment: ostracods, bivalves and shrimp-like arthropods

728 (Pygocephalomorpha) first adapted to freshwater in the early Carboniferous (Gray, 1988;

729 Bennett, 2008; Bennett et al., 2012) and were a key part of the food chain. Actinopterygians,

30

730 rhizodonts, dipnoans, tetrapods, acanthodians and elasmobranch chondrichthyans also thrived

731 in these early Carboniferous freshwater-brackish environments (Friedman and Sallan, 2012;

732 Gray, 1988).

733   The extinction of plant groups including trees such as *Archaeopteris* at the

734 Hangenberg event affected the terrestrial landscape (Decombeix et al., 2011) and may have

735 driven the tetrapods from more fluvially dominated upper Famennian environments into the

736 Tournaisian seasonal wetland environments. The seasonal variability of such environments

737 and close juxtaposition of different habitats may have produced the conditions in which

738 previously aquatic tetrapods adapted to the more terrestrial realm.

739 **6. Conclusions**

740   The Ballagan Formation of northern Britain provides a window into an environment

741 soon after the Late-Devonian mass extinction, where early Carboniferous tetrapods were

742 known to have been living. The formation comprises a 500 m thick sandstone – siltstone –

743 cementstone succession containing 298 palaeosols described from three sites. The palaeosols

744 are divided into four pedotypes, interpreted to be: Entisols, Inceptisols, gleyed Inceptisols and

745 Vertisols. This study records in detail one of the thickest and most complete successions of

746 palaeosols from the Tournaisian. Rooting is abundant through all the palaeosols, from

747 shallow root mats and thin hair-like root traces to the thicker root traces typical of arborescent

748 lycopods. A floodplain with diverse soil types and vegetation is inferred.

749   The groundwater table varied widely as shown by the different palaeosols and their

750 geochemistry and was affected by high evaporation rates. The presence of deep vertic cracks

751 and evaporite deposits are indicative of high mean annual rainfall and variable soil

752 alkalinities alternating with periods of wetting and drying. This wet to dry switching suggests

753 a sharply contrasting seasonal climate.

31

754   The palaeosols provide a unique insight into an early Carboniferous tropical coastal

755   floodplain and its tetrapod habitats. The move of tetrapods from the uppermost Famennian

756   aquatic forms to the more terrestrially capable Tournaisian forms occurred in a seasonally

757   changeable environment. The close juxtaposition of a diverse array of habitats may have been

758   a driver in the evolution and radiation of tetrapods into the terrestrial realm.

768   **References**

769   Adams, J.S., Kraus, M.J., Wing, S.L., 2011. Evaluating the use of weathering indices for

770   determining mean annual precipitation in the ancient stratigraphic record. Palaeogeography,

771   Palaeoclimatology, Palaeoecology 309, 358-366.

772   Algeo, T.J., Scheckler, S.E., 1998. Terrestrial-marine teleconnections in the Devonian: links

773   between the evolution of land plants, weathering processes, and marine anoxic events.

774   Philosophical Transactions of the Royal Society B: Biological Sciences 353, 113-130.

775   Alonso-Zarza, A.M., Wright, V.P., 2010. Calcretes. In: Alonso-Zarza, A.M., Tanner, L.H.

776   (eds.), Carbonates in continental settings: Geochemistry, Diagenesis and Applications.

777   Elsevier, pp. 177-224.

778   Anderson, J., Smithson, T., Mansky, C., Meyer, T., Clack, J., 2015. A diverse tetrapod fauna

779   at the base of 'Romer's Gap'. PloS ONE 10(4), 1-27. http://dx.doi.org/10.1371/pone.0125446.

780   Anderton, R., 1985. Sedimentology of the Dinantian of Foulden, Berwickshire, Scotland.

781   Transactions of the Royal Society of Edinburgh: Earth Sciences 76, 7-12.

782   Andrews, J.E., Nabi, G., 1998. Palaeoclimatic significance of calcretes in the Dinantian of the

783   Cockburnspath Outlier (East Lothian-North Berwickshire). Scottish Journal of Geology 34,

784   153-164.

785   Andrews, J.E., Turner, M.S., Nabi, G., Spiro, B., 1991. The anatomy of an early Dinantian

786   terraced floodplain: palaeo-environment and early diagenesis. Sedimentology 38, 271-287.

787   Astin, T., Marshall, J., Blom, H., Berry, C., 2010. The sedimentary environment of the Late

788   Devonian East Greenland tetrapods. In: The terrestrialization process; modelling complex

789   interactions at the biosphere-geosphere interface. Geological Society, London, Special

790   Publication 339, 93-109.

33

791   Barnett, A.J., Wright, V.P., Crowley, S.F., 2012, Recognition and significance of paludal

792   dolomites: LateMississippian, Kentucky, USA. International Association of Sedimentologists

793   Special Publication 45, 477-500.

794   Bashforth, A.R., Cleal, C.J., Gibling, M.R., Falcon-Lang, H.J., Miller, R.F., 2014.

795   Paleoecology of Early Pennsylvanian vegetation on a seasonally dry tropical landscape

796   (Tynemouth Creek Formation, New Brunswick, Canada). Review of Palaeobotany and

797   Palynology 200, 229-263.

798   Belt, E.S., Freshney, E.C., Read, W.A., 1967. Sedimentology of Carboniferous cementstone

799   facies, British Isles and eastern Canada. The Journal of Geology 75, 711-721.

800   Bennett, C., 2008. A review of the Carboniferous colonisation of non-marine environments

801   by ostracods. Senckenbergiana lethaea 88, 37-46.

802   Bennett, C.E., Siveter, D.J., Davies, S.J., Williams, M., Wilkinson, I.P., Browne, M., Miller,

803   C.G., 2012. Ostracods from freshwater and brackish environments of the Carboniferous of

804   the Midland Valley of Scotland: the early colonization of terrestrial water bodies. Geological

805   Magazine 149, 366-396.

806   Bennett, C.E., Kearsey, T., Davies, S.J., Millward, D., Clack, J., Smithson, T., Marshall,

807   J.E.A., 2016. Early Carboniferous sandy siltstones preserve rare vertebrate fossils in seasonal

808   flooding episodes. Sedimentology.

809   http://dx.doi.org/10.1111/sed.12280.DOI: 10.1111/sed.12280.

810   Bown, T.M., Kraus, M.J., 1987. Integration of channal and floodplain suites: I.

811   Developmental sequence and lateral relations of alluvial paleosols. Journal of Sedimentary

812   Petrology 57, 587-601.

813   Breecker, D., Sharp, Z., McFadden, L.D., 2009. Seasonal bias in the formation and stable

814   isotopic composition of pedogenic carbonate in modern soils from central New Mexico,

815   USA. Geological Society of America, Bulletin 121, 630-640.

816   Browne, M.A.E., Dean, M.T., Hall, I.H.S., McAdam, A.D., Monro, S.K., Chisholm, J.I.,

817   1999. A lithostratigraphical framework for the Carboniferous rocks of the Midland Valley of

818   Scotland. British Geological Survey Research Report RR/99/07.

819   Campbell, K.S.W., Bell, M.W., 1977. A primitive amphibian from the Late Devonian of New

820   South Wales. Alcheringa, 1, 369-381.

821   Caudill, M.R., Driese, S.G., Mora, C.I., 1996. Preservation of a paleo-Vertisol and an

822   estimate of late Mississippian paleoprecipitation. Journal of Sedimentary Research 66, 58-70.

823   Clack, J.A., 1997. Devonian tetrapod trackways and trackmakers; a review of the fossils and

824   footprints. Palaeogeography, Palaeoclimatology, Palaeoecology 130, 227-250.

825   Clack, J.A., 2002. An early tetrapod from `Romer's Gap'. Nature 418, 72-76.

826   Clack, J. A., 2009. The fin to limb transition: new data, interpretations, and hypotheses from

827   paleontology and developmental biology. Annual Review of Earth and Planetary Sciences 37,

828   163-179.

829   Cressler, W.L. III, Daeschler, E.B., Slingerland, R., Peterson, D.A., 2010. Terrestrialization

830   in the Late Devonian: a palaeoecological overview of the Red Hill site, Pennsylvania, USA.

831   In: Clement, G., Vecoli, M. (Eds.), The terrestrialization process: modelling complex

832   interaction at the biosphere-geosphere interface. Geological Society, London, Special

833   Publication 339, 111-128.

834   Daeschler, E.B., Cressler, W.L. III, 2011. Late Devonian paleontology and

835   paleoenvironments at Red Hill and other fossil sites in the Catskill Formation of north-central

836   Pennsylvania. In: Ruffolo, R.M., Caimpaglio, C.N. (Eds.), From the Shield to the Sea:

837   Geological Trips from the 2011 Joint Meeting of the GSA Northeastern and North-Central

838   Section. Geological Society of America, Field Guide 20, pp. 1-16.

839   Decombeix, A-L., Meyer-Berthaud, B. Galtier, J. 2011. Transitional changes in arborescent

840   lignophytes at the Devonian–Carboniferous boundary. Journal of the Geological Society,

841   London 168, 547-557.

842   Driese, S.D., 2004. Pedogenic translocation of Fe in modern and ancient Vertisols and

843   implications for interpretations of the Hekpoort paleosol (2.25 Ga). Journal of Geology 112,

844   543-560.

845   Driese, S.G., Mora, C.I., Stiles, C.A., Joeckel, R., Nordt, L.C., 2000. Mass-balance

846   reconstruction of a modern Vertisol: implications for interpreting the geochemistry and burial

847   alteration of paleo-Vertisols. Geoderma 95, 179-204.

848   Falcon-Lang, H.J., 1999. The Early Carboniferous (Courceyan–Arundian) monsoonal climate

849   of the British Isles: evidence from growth rings in fossil woods. Geological Magazine 136,

850   177-187.

851   Falcon-Lang, H.J., 2004. Early Mississippian lycopsid forests in a delta-plain setting at

852   Norton, near Sussex, New Brunswick, Canada. Journal of the Geological Society, London

853   161, 969-981.

854   Falcon-Lang, H.J., Jud, N.A., Nelson, W.J., DiMichele, W.A., Chaney, D.S., Lucas, S.G.,

855   2011. Pennsylvanian coniferopsid forests in sabkha facies reveal the nature of seasonal

856   tropical biome. Geology 39, 371-374.

857   Friedman, M. Sallan, L. C., 2012. Five hundred million years of extinction and recovery: a

858   Phanerozoic survey of large-scale diversity patterns in fishes. Palaeontology 55, 707-742.

859   Garcia, W.J., Storrs, G.W., Greb, S.F., 2006. The Hancock County tetrapod locality: A new

860   Mississippian (Chesterian) wetlands fauna from western Kentucky (USA). Geological

861   Society of America, Special Papers 399, 155-167.

862   Gastaldo, R.A., 1986. Implications on the paleoecology of autochthonous lycopods in clastic

863   sedimentary environments of the Early Pennsylvanian of Alabama. Palaeogeography,

864   Palaeoclimatology, Palaeoecology 53, 191-212.

865   Gordon, C., Ntiamoa-Baidu, Y., Ryan, J.M., 2000. The Muni-Pomadze Ramsar site.

866   Biodiversity & Conservation 9(4), 447-464.

867   Graham, J.R., 1981. Fluvial sedimentation in the Lower Carboniferous of Clew Bay, County

868   Mayo, Ireland. Sedimentary Geology 30, 195-211.

869   Gray, J., 1988. Evolution of the freshwater ecosystem: the fossil record. Palaeogeography,

870   Palaeoclimatology, Palaeoecology 62, 1-214.

871   Greb, S.F., DiMichele, W.A., Gastaldo, R.A., 2006. Evolution and importance of wetlands in

872   earth history, In: Greb, S.F., DiMichele, W.A. (Eds.), Wetlands through time. Geological

873   Society of America, Special Paper 399, 1-40.

874   Harrington, G.J., Kemp, S.J., Koch, P.L., 2004. Palaeocene–Eocene paratropical floral

875   change in North America: responses to climate change and plant immigration. Journal of the

876   Geological Society, London 161, 173-184

877   Jarecki, L., Walkey, M., 2006. Variable hydrology and salinity of salt ponds in the British

878   Virgin Islands. Saline Systems 2(2), 1-15. http://dx.doi.org/10.1186/1746-1448-2-2.

879   Joeckel, R., Clement, B.A., 2005. Soils, surficial geology, and geomicrobiology of saline-

880   sodic wetlands, North Platte River Valley, Nebraska, USA. Catena 61, 63-101.

881   Kaiser, S. I., Aretz, M., Becker, R. T., 2015. The global Hangenberg Crisis (Devonian–

882   Carboniferous transition): review of a first-order mass extinction. Geological Society,

883   London, Special Publications 423, 423-9.

884   Krasilnikov, P., Calderón, N. E. G., 2006. A WRB-based buried paleosol classification.

885   Quaternary International, 156, 176-188.

886   Kraus, M.J., 1999. Paleosols in clastic sedimentary rocks: their geologic applications. Earth

887   Science Reviews 47, 41-70.

888   Kraus, M.J., Hasiotis, S.T., 2006. Significance of different modes of rhizolith preservation to

889   interpreting paleoenvironmental and paleohydrologic settings: Examples from Paleogene

890   paleosols, Bighorn Basin, Wyoming, U.S.A. Journal of Sedimentary Research 76, 633-646.

891   Lucas, S.G., 2015. *Thinopus* and a critical review of Devonian tetrapod footprints. Ichnos, 22,

892   136-154.

893   Machette, M.N., 1985. Calcic soils of the southwestern United States. Geological Society of

894   America, Special Papers 203, 1-22.

895   Mack, G. H., James, W. C. and Monger, H. C., 1993. Classification of paleosols. Geological

896   Society of America, Bulletin, 105: 129-136.

897   Mack, G., James, W. C., 1994. Paleoclimate and the global distribution of paleosols.

898   Journal of Geology, 102: 360-366.

899   Marshall, J.E.A., Haughton, P.D.W., Hillier, S.J., 1994. Vitrinite reflectivity and the structure

900   and burial history of the Old Red Sandstone of the Midland Valley of Scotland. Journal of the

901   Geological Society, London 151, 425-438.

902   Merriman, R., Kemp, S., 1996. Clay minerals and sedimentary basin maturity. Mineralogical

903   Society, Bulletin 111, 7-8.

904   Moore, T.E., Nilsen, T.H., 1984. Regional variations in the fluvial Upper Devonian and

905   Lower Mississippian (?) Kanayut Conglomerate, Brooks Range, Alaska. Sedimentary

906   geology 38, 465-497.

907   Myers, T.S., Tabor, N.J., Rosenau, N.A., 2014. Multiproxy approach reveals evidence of

908   highly variable paleoprecipitation in the Upper Jurassic Morrison Formation (western United

909   States). Geological Society of America, Bulletin 126, 1105-1116.

910   Narkiewicz, M., Ahlberg, P.E., 2010. Tetrapod trackways from the early Middle Devonian

911   period of Poland. Nature 463, 44-48.

912   Narkiewicz, M., Grabowski, J., Narkiewicz, K., Niedźwiedzki, G., Retallack, G.J., Szrek, P.,

913   De Vleeschouwer, D., 2015. Palaeoenvironments of the Eifelian dolomites with earliest

914   tetrapod trackways (Holy Cross Mountains, Poland). Palaeogeography, Palaeoclimatology,

915   Palaeoecology 420, 173-192. http://dx.doi.org/10.1016/j.palaeo.2014.12.013.

916   Nettleton, W. D., Brasher, B. R., Benham, E. C., Ahrens, R. J., 1998. A classification system

917   for buried paleosols. Quaternary International 51, 175-183.

918   Nettleton, W. D., Olson, C. G. and Wysocki, D. A., 2000. Paleosol classification: problems

919   and solutions. Catena 41, 61-92.

920   Niklas, K.J., 1994. Plant allometry. University of Chicago Press, Chicago.

921   Niedzwiedzki, G., Szrek, Narkiewicz, P.K., Nordt, L., Driese, S., 2010. New weathering

922   index improves paleorainfall estimates from Vertisols. Geology 38, 407-410.

923   Paton, R.L., Smithson, T.R., Clack, J.A., 1999. An amniote-like skeleton from the Early

924   Carboniferous of Scotland. Nature 398, 508-513.

925   Peel, M.C., Finlayson, B.L., McMahon, T.A., 2007. Updated world map of the Köppen-

926   Geiger climate classification. Hydrology and Earth System Sciences Discussions, European

927   Geosciences Union 11, 1633-1644.

928   Pfefferkorn, H., Fuch, K., 1991. A field classification of fossil plant substrate interactions.

929   Neues Jahrbuch für Geologie und Paläontologie - Abhandlungen 183, 17-36.

930   Pierce, S.E., Clack, J.A., Hutchinson, J.R., 2012. Three-dimensional limb joint mobility in

931   the early tetrapod Ichthyostega. Nature 486, 523-526.

932   Quast, A., Hoefs, J., Paul, J., 2006. Pedogenic carbonates as a proxy for palaeo-CO_2 in the

933   Palaeozoic atmosphere. Palaeogeography, Palaeoclimatology, Palaeoecology 242, 110-125.

934   Raven, J., Edwards, D., 2001. Roots: evolutionary origins and biogeochemical significance.

935   Journal of Experimental Botany 52, 381-401.

936   Raymond, A. Lambert, L., Costanza, S. Slone, E.J., Cutlip, P.C., 2010. Cordaiteans in

937   paleotropical wetlands: An ecological re-evaluation. International Journal of Coal Geology

938   83, 248-265.

939   Retallack, G. J., 1988. Field recognition of paleosols. Geological Society of America, Special

940   Papers 216, 1-20.

941   Retallack, G. J., 1993. Classification of palaeosols: discussion. Geological Society of

942   America, Bulletin 105, 383-400.

943   Retallack, G. J., 1994. The environmental factor approach to the interpretation of palaeosols.

944   In: Amundson, R., Harden, J., Singer, M. (Eds.), Factors in soil formation: and fiftieth

945   anniversary retrospective. Soil Science Society of America, Special Publication 33, 31-64.

946   Retallack, G.J., 1997. Colour guide to paleosols. Wiley & Sons Ltd.

947   Retallack, G.J., 1998. Fossil soils and completeness of the rock and fossil record. In:

948   Donovan, S.K., Paul, C.R.R. (Eds.), The adequacy of the fossil record, Wiley & Sons Ltd.

949   Retallack, G. J., 2011. Woodland hypothesis for Devonian tetrapod evolution. The Journal of

950   Geology 119, 235-258.

951   Retallack, G., Catt, J., Chaloner, W., 1985. Fossil soils as grounds for interpreting the advent

952   of large plants and animals on land [and discussion]. Philosophical Transactions of the Royal

953   Society B: Biological Sciences 309, 105-142.

954   Retallack, G.J., Dilcher, D.L., 1988. Reconstructions of selected seed ferns. Annals of the

955   Missouri Garden 75, 1010-1057.

956   Retallack, G.J., Huang, C., 2011. Ecology and evolution of Devonian trees in New York,

957   USA. Palaeogeography, Palaeoclimatology and Palaeoecology 299, 110-128.

958   Retallack, G.J., Hunt, R.R., White, T.E., 2009. Late Devonian tetrapod habitats indicated by

959   palaeosols in Pennsylvania. Journal of the Geological Society, London 166, 1143-1156.

960   Reynolds Jr. R.C., Reynolds III, R.C., 2013. Description of Newmod II™. The calculation of

961   one-dimensional X-ray diffraction patterns of mixed layered clay minerals. R C Reynolds III,

962   1526 Farlow Avenue, Crofton, MD 21114.

963   Rust, B.R., Nanson, G.C., 1989. Bedload transport of mud as pedogenic aggregates in

964   modern and ancient rivers. Sedimentology 36, 291-306.

965   Rygel, M.C., Calder, J.H., Gibling, M.R., Gingras, M.K., Melrose, C.S., 2006. Tournaisian

966   forested wetlands in the Horton Group of Atlantic Canada. Geological Society of America,

967   Special Papers 399, 103-126.

968   Scotese, C.R., McKerrow, W.S., 1990. Revised world maps and introduction. Geological

969   Society, London, Memoirs 12, 1-21.

970   Scott, W.B., 1986. Nodular carbonates in the Lower Carboniferous, Cementstone Group of

971   the Tweed embayment, Berwickshire: evidence for a former sulphate evaporite. Scottish

972   Journal of Geology 22, 325-345.

973   Sheldon, N.D., 2005. Do red beds indicate paleoclimatic conditions? : A Permian case study.

974   Palaeogeography, Palaeoclimatology, Palaeoecology 228, 305-319.

975   Sheldon, N.D., Retallack, G.J., Tanaka, S., 2002. Geochemical climofunctions from North

976   America soils and application to paleosols across the Eocene-Oligocene boundary in Oregon.

977   Journal of Geology 110, 687-696.

978   Sheldon, N.D., Tabor, N.J., 2009. Quantitative paleoenvironmental and paleoclimatic

979   reconstruction using paleosols. Earth Science Reviews 95, 1-52.

980   Soil Survey Staff, 1999. Soil Taxonomy: A basic system of soil classification for making and

981   interpreting soil surveys, agriculture handbook number 436. United States Department of

982   Agriculture Natural Resources Conservation Service. 871 pp.

983   Smithson, T.R., Wood, S.P., Marshall, J.E.A., Clack, J.A., 2012. Earliest Carboniferous

984   tetrapod and arthropod faunas from Scotland populate Romer's Gap. Proceedings of the

985   National Academy of Sciences 109, 4532-4537.

986   Stephenson, M.H., Williams, M., Monaghan, A.A., Arkley, S., Smith, R.A., 2002.

987   Biostratigraphy and palaeoenvironments of the Ballagan Formation (Lower Carboniferous) in

988   Ayrshire. Scottish Journal of Geology 38, 93-111.

989   Stephenson, M.H., Williams, M., Leng, M.J., Monaghan, A.A., 2004a. Aquatic plant

990   microfossils of probable non-vascular origin from the Ballagan Formation (Lower

991   Carboniferous), Midland Valley, Scotland. Proceedings of the Yorkshire Geological Society

992   55, 145-158.

993   Stephenson, M.H., Williams, M., Monaghan, A.A., Arkley, S., Smith, R.A., Dean, M.,

994   Browne, M.A.E., Leng, M., 2004b. Palynomorph and ostracod biostratigraphy of the

995   Ballagan Formation, Midland Valley of Scotland, and elucidation of intra-Dinantian

996   unconformities. Proceedings of the Yorkshire Geological Society 55, 131-143.

997   Tabor, N.J., Yapp, C.J., Montañez, I.P., 2004. Goethite, calcite, and organic matter from

998   Permian and Triassic soils: carbon isotopes and CO_2 concentrations 1. Geochimica et

999   Cosmochimica Acta 68, 1503-1517.

1000   Turner, M.S., 1991. Geochemistry and diagenesis of basal Carboniferous dolostones from

1001   southern Scotland. Unpublished Ph. D. thesis, University of East Anglia.

1002   Ward, P., Labandeira, C., Laurin, M., Berner, R.A., 2006. Confirmation of Romer's Gap as a

1003   low oxygen interval constraining the timing of initial arthropod and vertebrate

1004   terrestrialization. Proceedings of the National Academy of Sciences 103, 16818-16822.

1005   Waters, C.N., 2011. A revised correlation of Carboniferous rocks in the British Isles.

1006   Geological Society of London, Special Reports 26, pp190.

1007   Williams, M., Stephenson, M.H., Wilkinson, I.P., Leng, M.J., Miller, C.G., 2005. Early

1008   Carboniferous (Late Tournaisian–Early Viséan) ostracods from the Ballagan Formation,

1009   central Scotland, UK. Journal of Micropalaeontology 24, 77-94.

1010   Wilson, M.J., 1999. The origin and formation of clay minerals in soils: past, present and

1011   future perspectives. Clay Minerals 34, 7-25.

1012   Wright, V., 1990. Equatorial aridity and climatic oscillations during the early Carboniferous,

1013   southern Britain. Journal of the Geological Society, London 147, 359-363.

1014   Wright, V., Vanstone, S., Robinson, D., 1991. Ferrolysis in Arundian alluvial palaeosols:

1015   evidence of a shift in the early Carboniferous monsoonal system. Journal of the Geological

1016   Society, London 148, 9-12.

1017   Wright, V.P., Tucker, M.E., 1991. Calcretes: an introduction. In: Wright, V.P., Tucker, M.E.,

1018   (Eds.) Calcretes. Blackwell Scientific Publications, Oxford, pp 1–22.

1019   Young, G.C., 2006. Biostratigraphic and biogeographic context for tetrapod origins during

1020   the Devonian: Australian evidence. Alcheringa: An Australasian Journal of Palaeontology,

1021   30, 409-428.

Table 1. Ballagan Formation pedotype classification

Palaeosol pedotype	Palaeosol horizon and thickness (cm)	Macromorphology	Classification	
			after USDA Soil Taxonomy	after Mack et al (1993)
Pe	A (5 - 35 cm)	Contains single tapering structures to branching and interlocking mats.	Entisol	Protosol
	C (2 - 18 cm)	Primary sedimentary lamination (cross bedding)		
Pi	(Eg) (1 - 30 cm) Present in 50% of this pedotype	Greenish grey to greyish green (5GY 5/1 to 5G 4/2). Internally massive and has an irregular boundary with the horizon below. Sinuous filamentous root traces and polygonal fractures.	Inceptisol	Protosol
	Bt (4 - 63 cm)	Reddish brown to red (2.5YR 6/3 to 10R 5/6). Extensive root traces which are preserved as drab root halos.		
	C (12 - 20 cm)	Bluish grey to dark reddish brown (10B 8/1 to 5YR 3/3). Disrupted primary sedimentary lamination.		
Pg	(O) (5 - 15 cm) Present in 11% of this pedotype	Black (N1), internally massive horizon with elevated TOC compared with rest of profile. Top surfaces commonly broken and brecciated.	gleyed Inceptisol	Gleysol
	(Eg) (2 - 45 cm)	Light greenish grey to light bluish grey (5BG 7/1 - 10BG 8/1). Internally massive and has an irregular boundary with the horizon below. Carbonised root traces and polygonal fractures.		
	Bg (10 - 73cm)	Light greenish grey to Light bluish grey (10G 8/1 - 10B 8/1). Yellow (2.5Y 7/6) mottles and contains nodules of ferro-siderite between 0.2 - 1 cm in diameter. Carbonised root traces.		
	C (3 - 23 cm)	Primary sedimentary lamination (cross-bedding). Some carbonised root traces.		
Pv	Eg (10 - 30 cm)	Dark greenish grey to pale green (5G 4/1 to 5G 6.2). Filamentous root traces preserved as carbon films.	Vertisol	Vertisol
	Bt (35 - 123 cm)	Dusky red to red (2.5YR 3/2 to 10R 5/6). Type H rooting structures preserved as drab root halos and minor pale green (5G 4/1) mottles.		
	(Bk) (5 - 15 cm)	Dusky red to red (2.5YR 3/2 to 10R 5/6). 0.5- 2cm in diameter and are of stage II carbonate nodules.		
	C (10 - 20 cm)	Dusky red (2.5YR 3/2). Primary sedimentary lamination.		
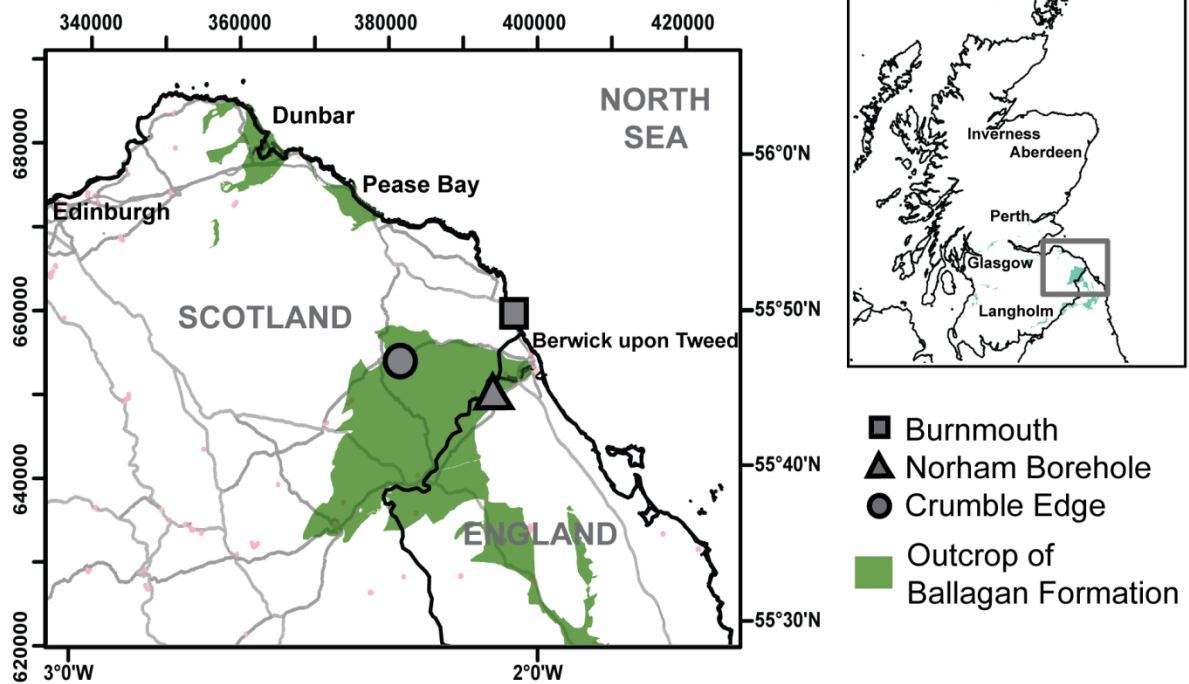
Fig. 1. Location of the field sections and borehole in this study; Burnmouth, Norham
borehole, Crumble Edge. The green area shows the outcrop of the Ballagan Formation, from
British Geological Survey DiGMapGB © NERC 2015. (contains Ordnance Survey data ©
Crown copyright and database right 2016).

1030

| PERIOD	STAGE	REGIONAL SUBSTAGE	PALYNOMORPH ZONE	LITHOSTRATIGRAPHY		
				Berwick-upon-Tweed	Langholm	
CARBONIFEROUS (MISSISSIPPIAN)	VISEAN	Holkerian	TS	Fell Sandstone Formation		Border Group
		Arundian	Pu			
		Chadian			Lyne Formation	Inverclyde Group
	TOURNAISIAN	Courceyan	CM	Ballagan Formation		
			VI	? ? ? ? Birrenswark and Kelso Volcanic Fms Kinnesswood Fm (Base not seen)		
DEV.	FAM.					
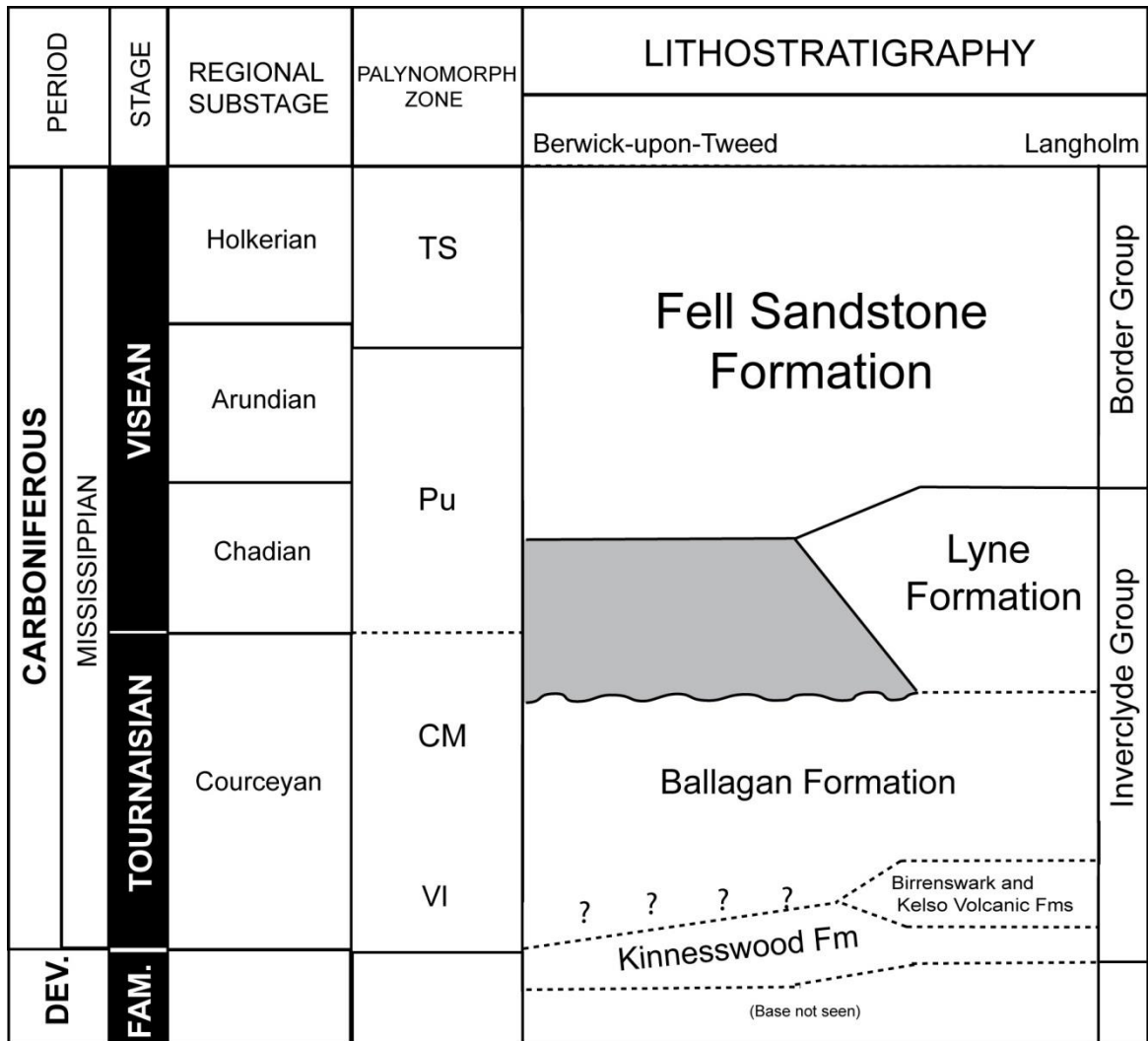
1031

1032 Fig. 2. Stratigraphic framework of the Scottish Borders and Northumberland basin (adapted
1033 from Waters, 2011). The zonal palynomorphs are VI = *Vallatisporites vallatus, Retusotriletes*
1034 *incohatus*; CM = *Schopfites claviger, Auroraspora macra*; Pu = *Lycospora pusilla*; TS =
1035 *Knoxisporites triradiatus, Knoxisporites stephanephorus.*

1036
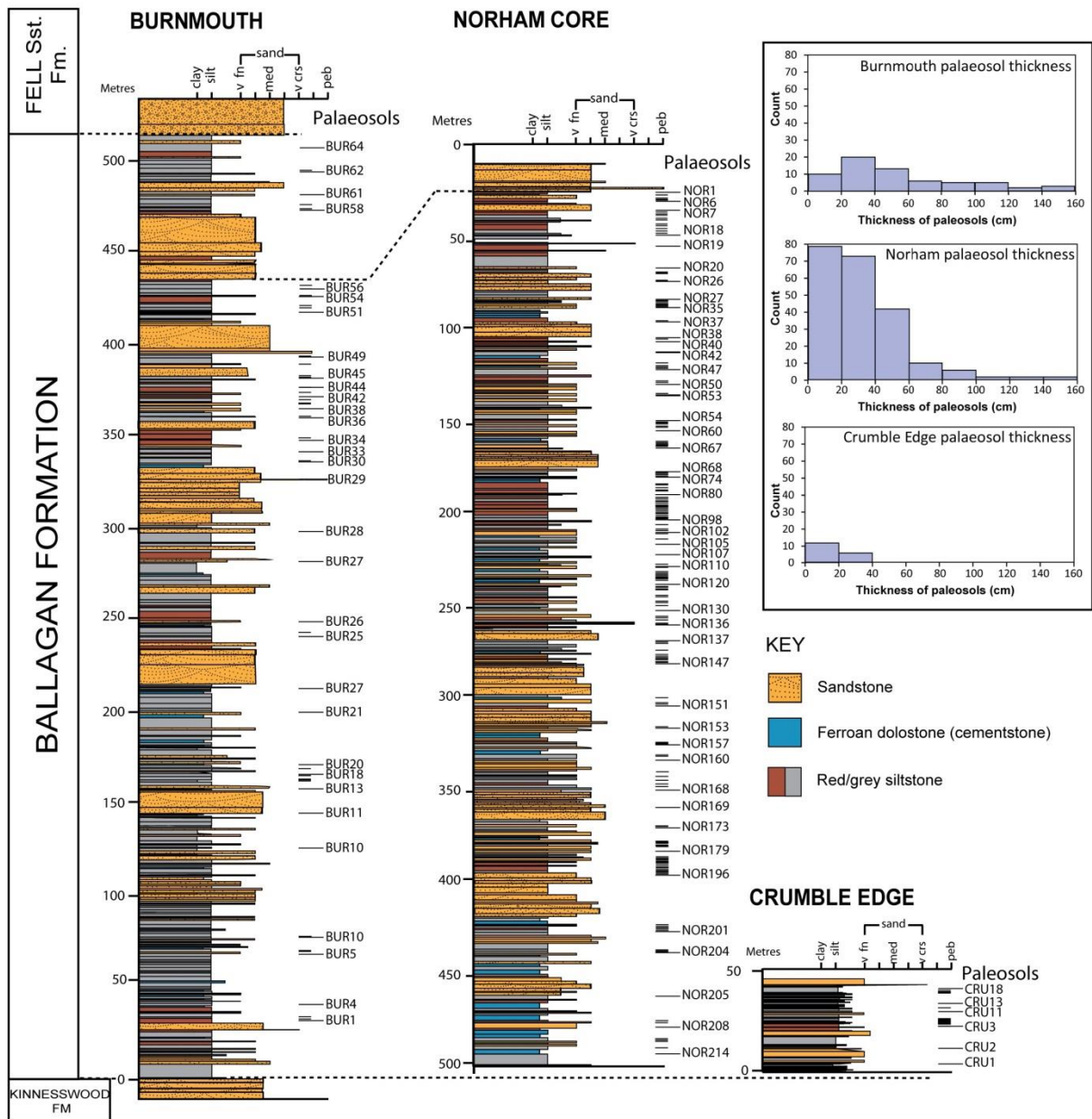
1039 Fig. 3. Sedimentary logs of sections in this study with locations of palaeosols marked. The
1040 box on the right shows histograms of the thickness of palaeosols at each section.

1041

48
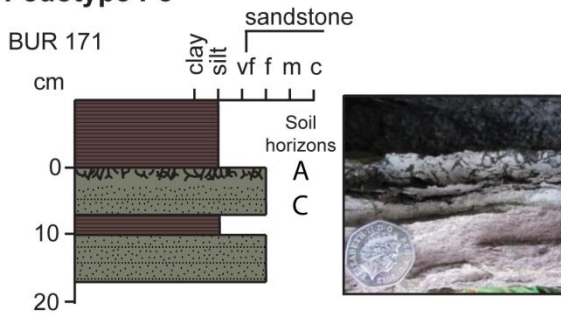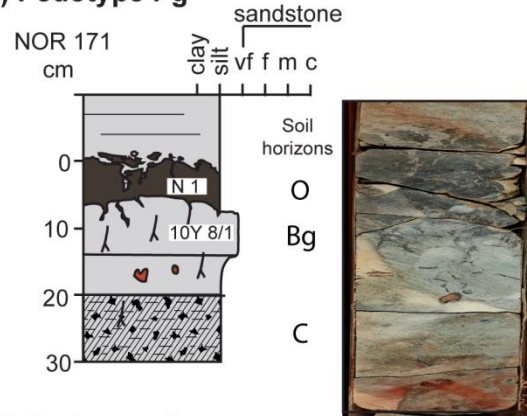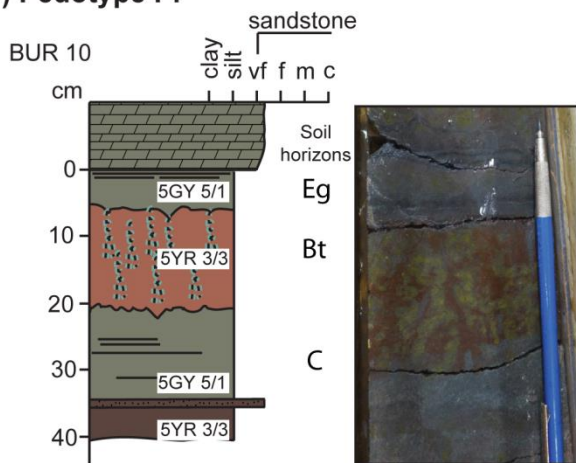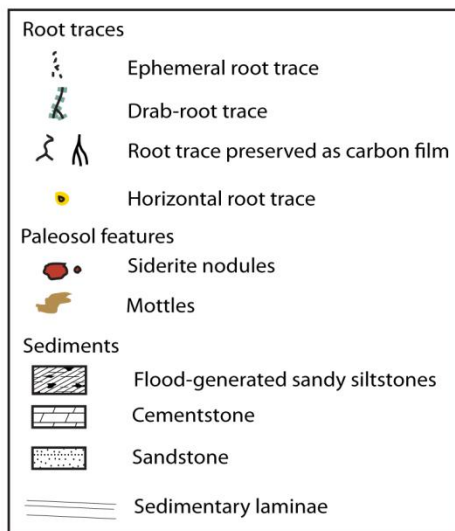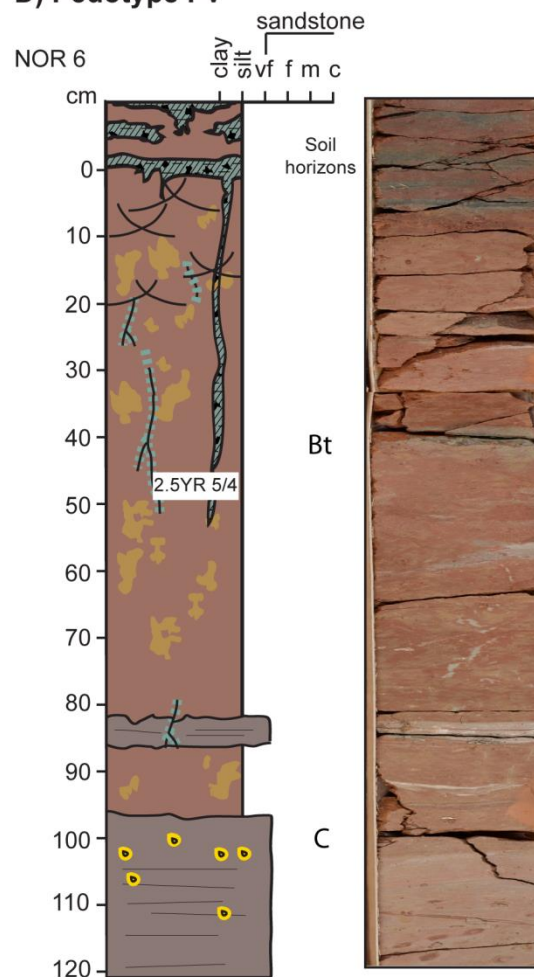
Fig. 4. Examples of the four pedotypes Pe, Pi, Pg and Pv. The core and field photos (on right in each example) illustrate the features recorded in the sedimentary logs (on left in each example). The numbers above the palaeosol (e.g., NOR 6) refer to the specific palaeosol horizon being used to typify that pedotype (see Appendix A). The soil horizons to the right of the logs are explained in the text. Munsell colours of each horizon are shown on the logs. Width of the core in photographs for B, C, D is 100 mm. Scale start at the top of the palaeosol.
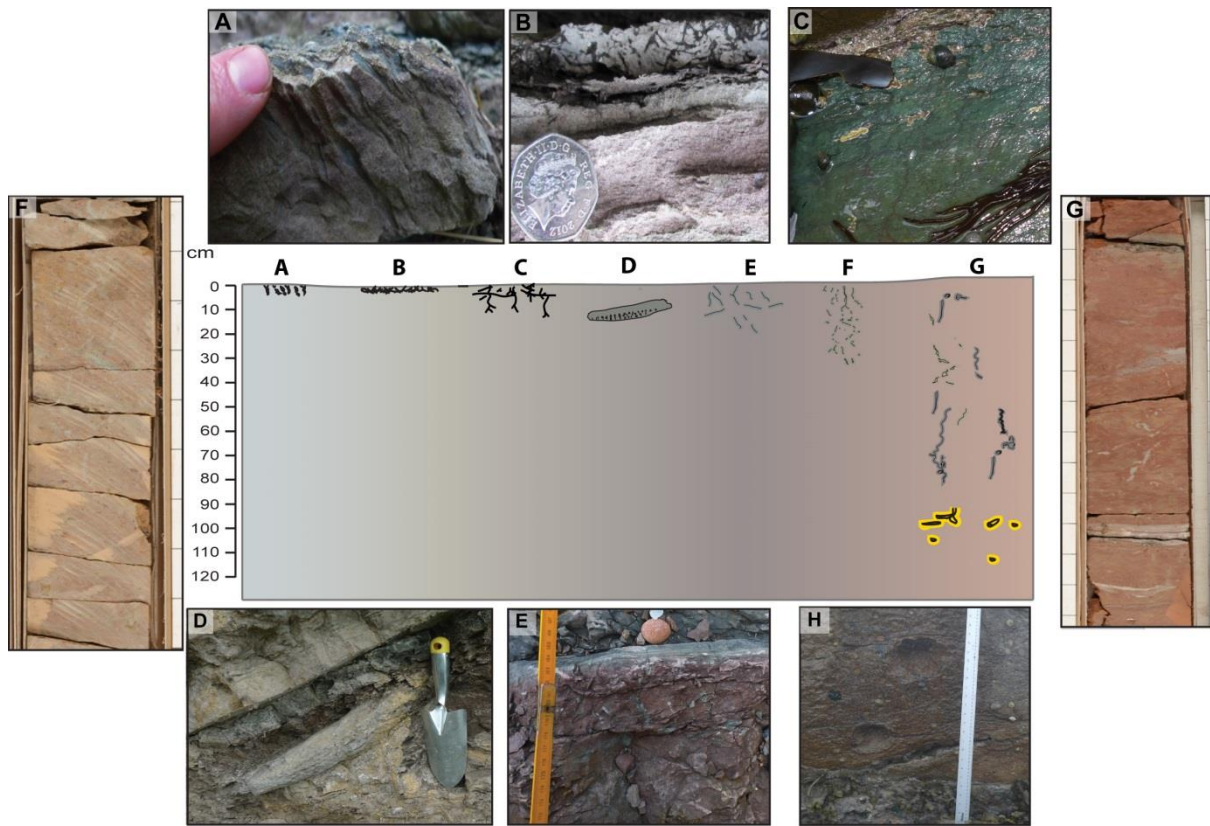
Fig. 5. Root traces found in the Ballagan Formation palaeosols. A) plug roots, B) rootmats, C) carbonized root traces with some lateral branches, D) lycopsid roots, E) drab root traces with some lateral branches, F) drab root linear traces with some bifurcation, G) linear traces with some bifurcation and horizontal roots at depth. H) in-situ tree stumps. The grey shade represents the degree to which the soil is gleyed.
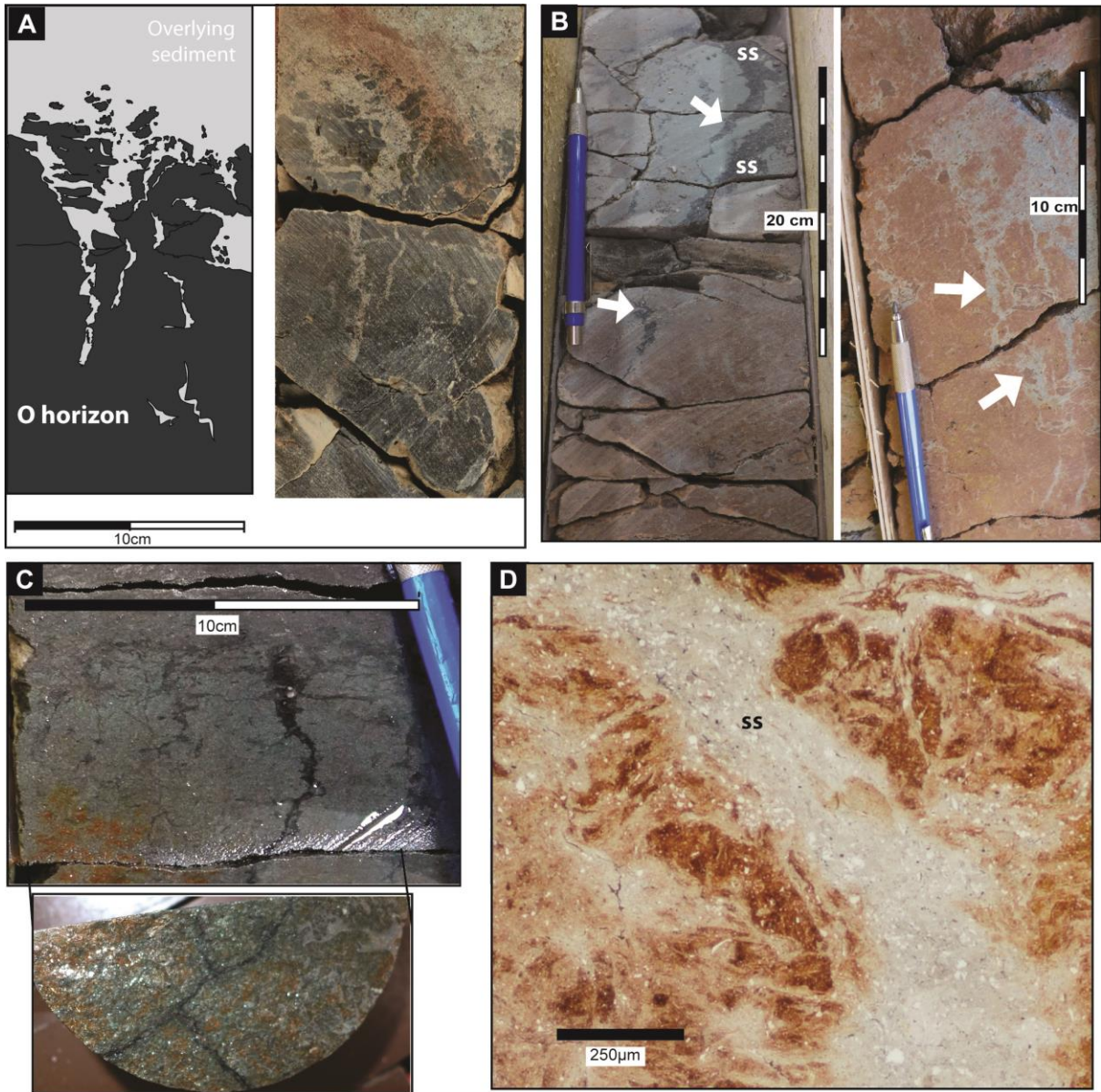
1058

1059 Fig. 6. Observed palaeosol crack types. A) Brecciation is observed to be associated only with,
1060 Pg: drawing (left) and core photograph (right). B) Deep penetrating cracks (arrowed) infilled
1061 with flood-generated sandy siltstones (ss) in pedotype Pv interpreted to be associated with
1062 gilgai micro-topography; C) Polygonal cracks in section (top) and plan view (bottom); D)
1063 Polygonal crack infilled with flood-generated sandy siltstone (ss) in a thin section
1064 photomicrograph of the same bed illustrated in C.

1065
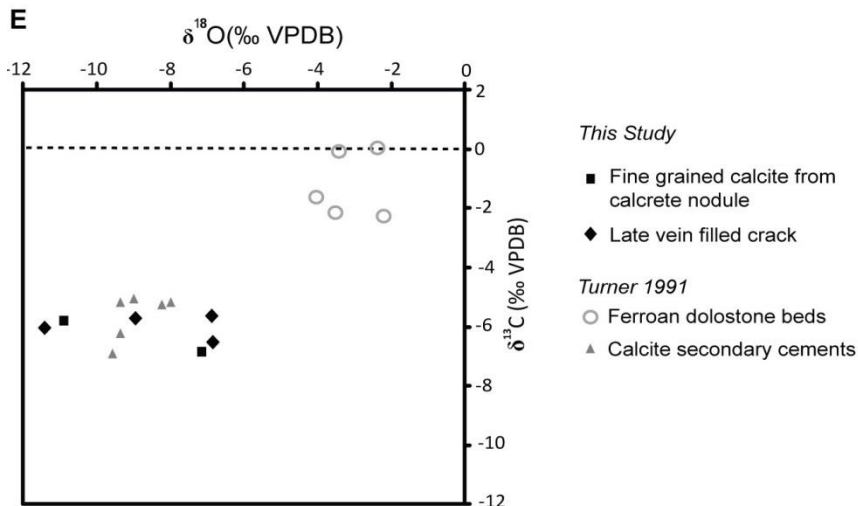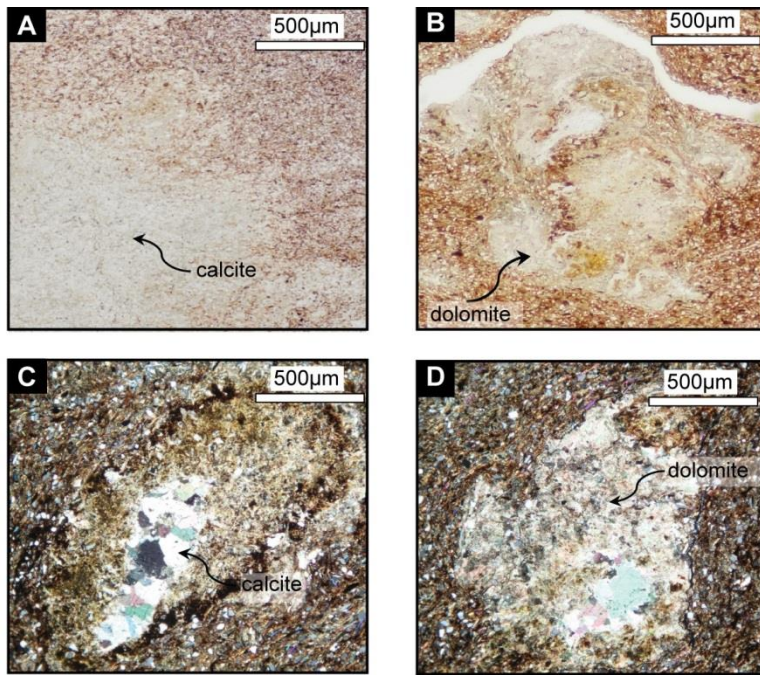
Fig. 7. Carbonate nodule micromorphology. A) Diffuse carbonate boundary of a nodule; B) fine mass of dolomite crystals surrounding larger crystals of calcite; C) Neomorphic replacement textures in centre of nodule; D) Carbonate nodule with diffuse boundaries in cross-polarised light showing sparry calcite core: E) Calcite isotope plot from palaeosol nodules from this study compared with results from Turner (1991) a representative data set of lacustrine dolomitic cementstones (homogeneous cementstone) and secondary calcite cements from Burnmouth.
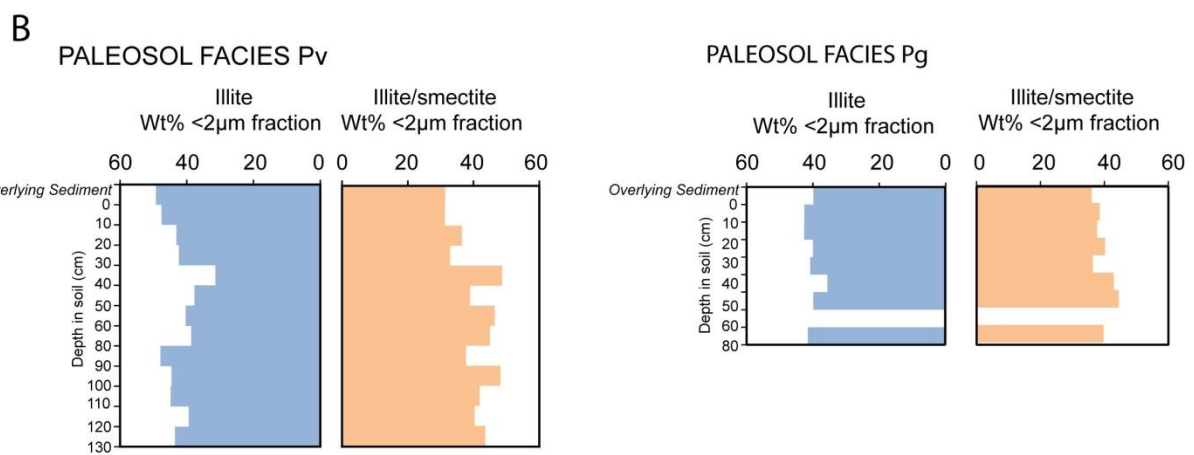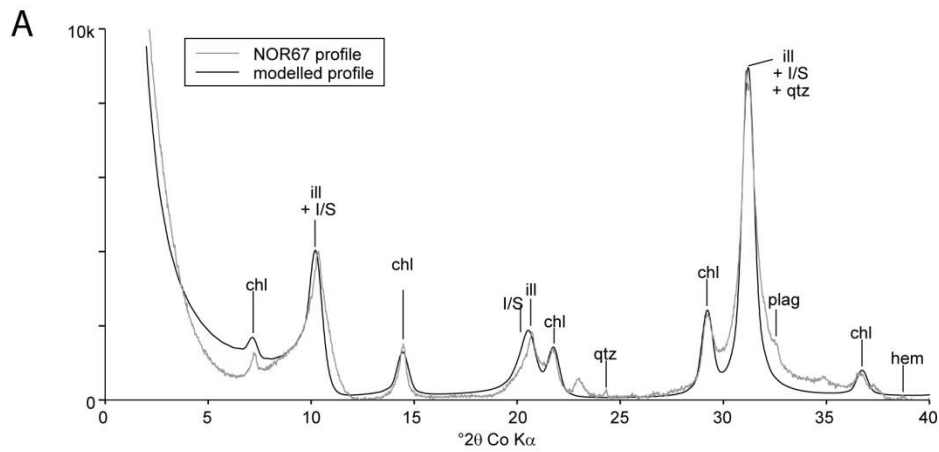
Fig. 8. A) Comparison of <2 μm ethylene glycol-solvated X-ray diffraction traces with NEWMOD II-modelled profile to illustrate excellent fit. B) The wt% values for illite and illite/smectite for all palaeosols of pedotype Pv and Pg analysed plotted against depth in soil in 10 cm bins (for results see Appendix B).
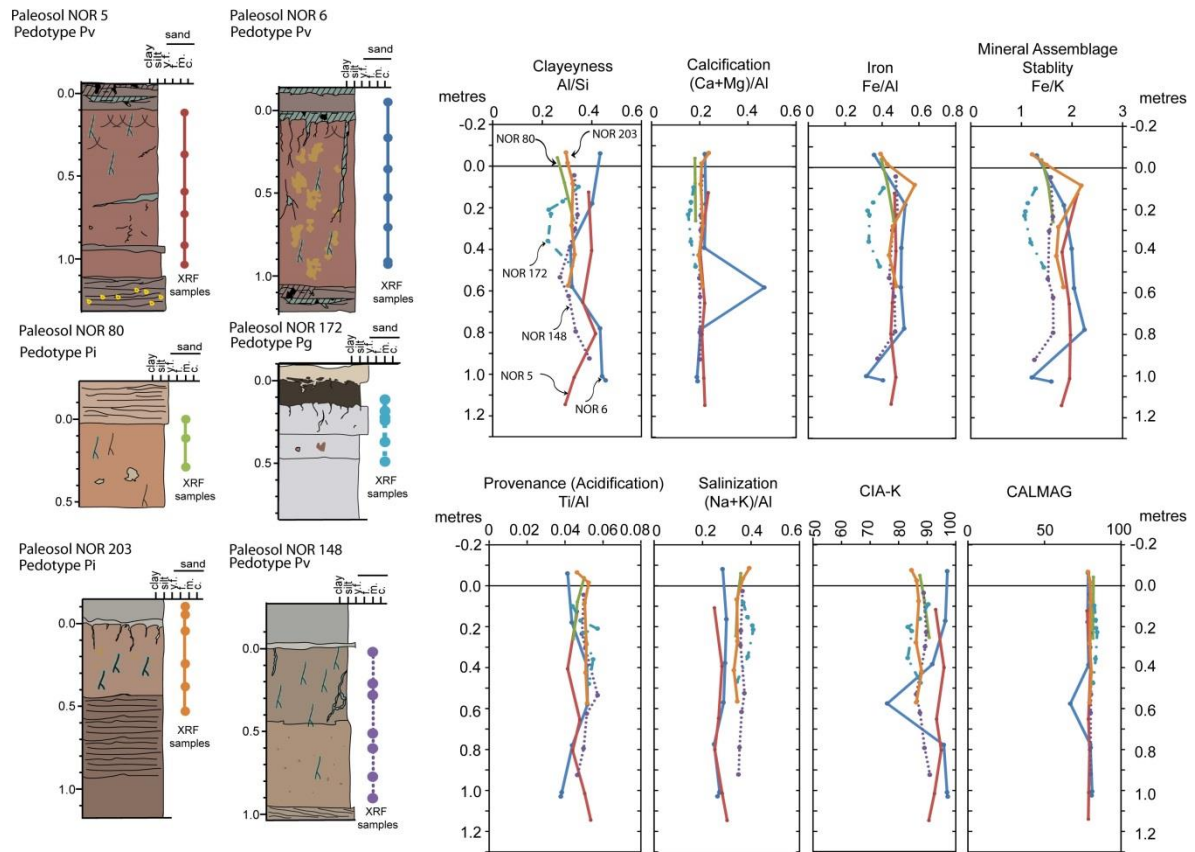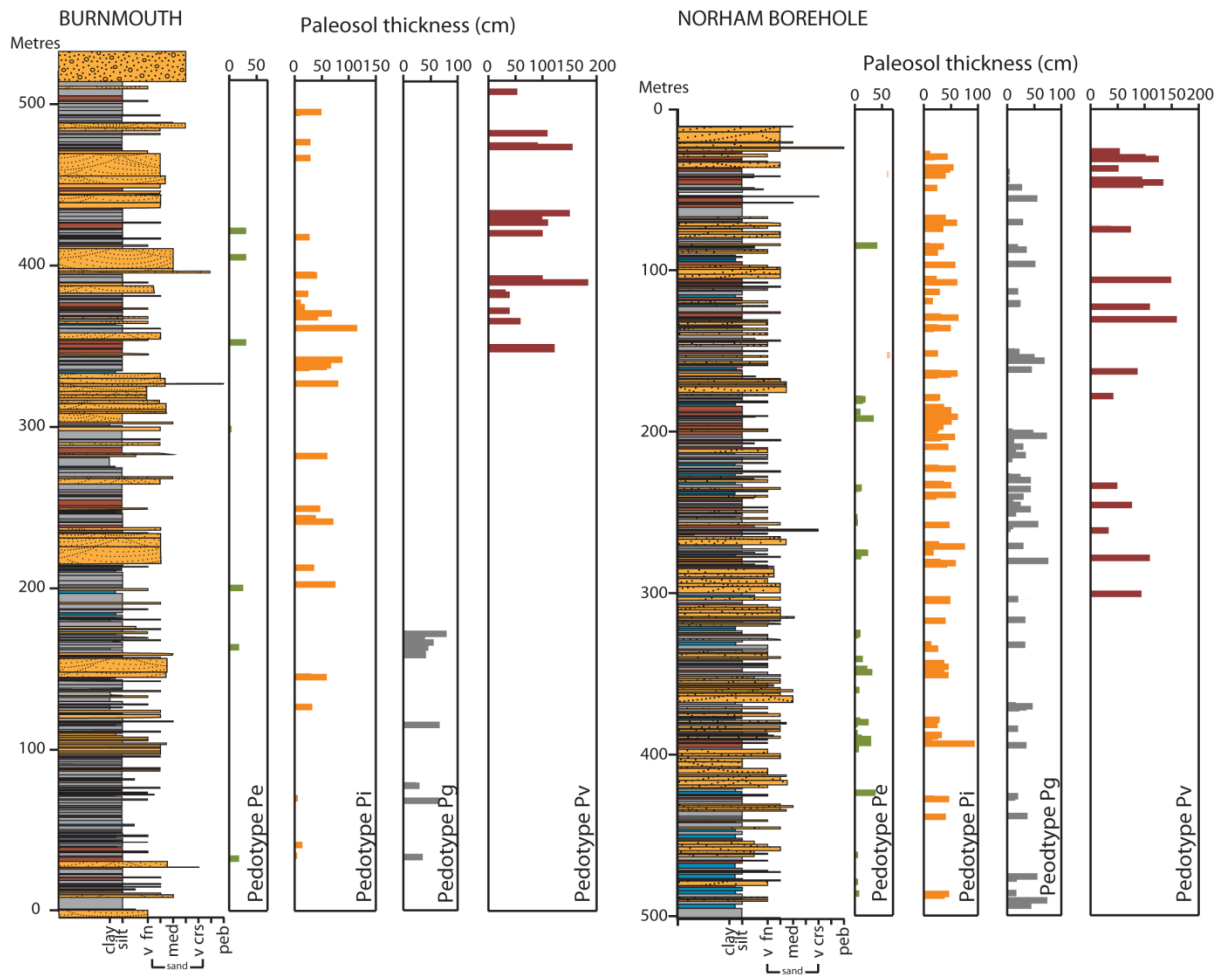
1081

1082 Fig. 9. Geochemical profiles for six palaeosols from the Norham core. Palaeosols NOR5,
1083 NOR6 and NOR149 are of pedotype Pv; NOR80 and NOR203 are of pedotype Pi and
1084 palaeosol NOR172 is of pedotype Pg (for key to sedimentary logs see Fig.4, (for results see
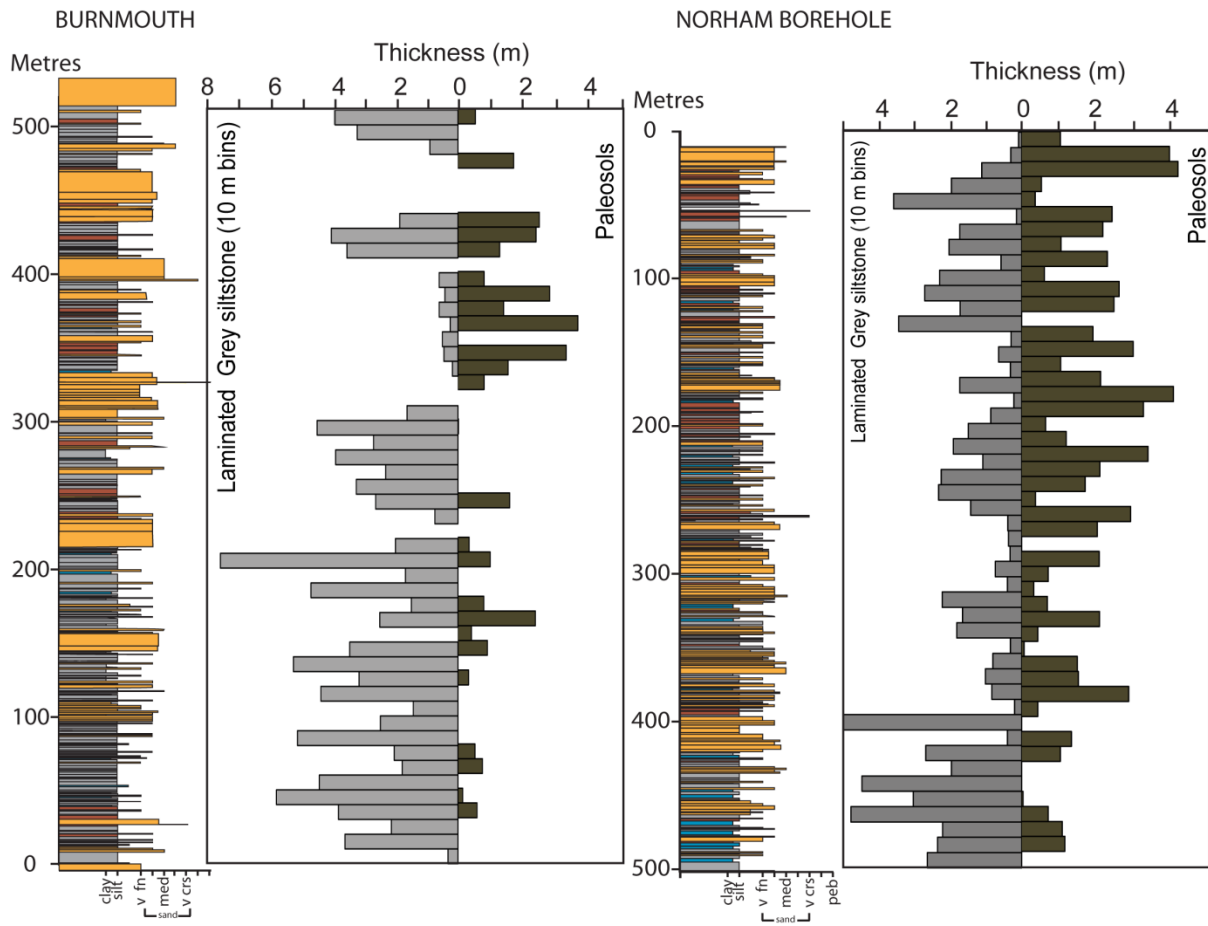1085 Appendix B).

1086

Fig. 10. Variation in thickness and distribution of the four pedotypes through the Burnmouth and in the Norham core sections (for key to sedimentary logs see Fig. 3).
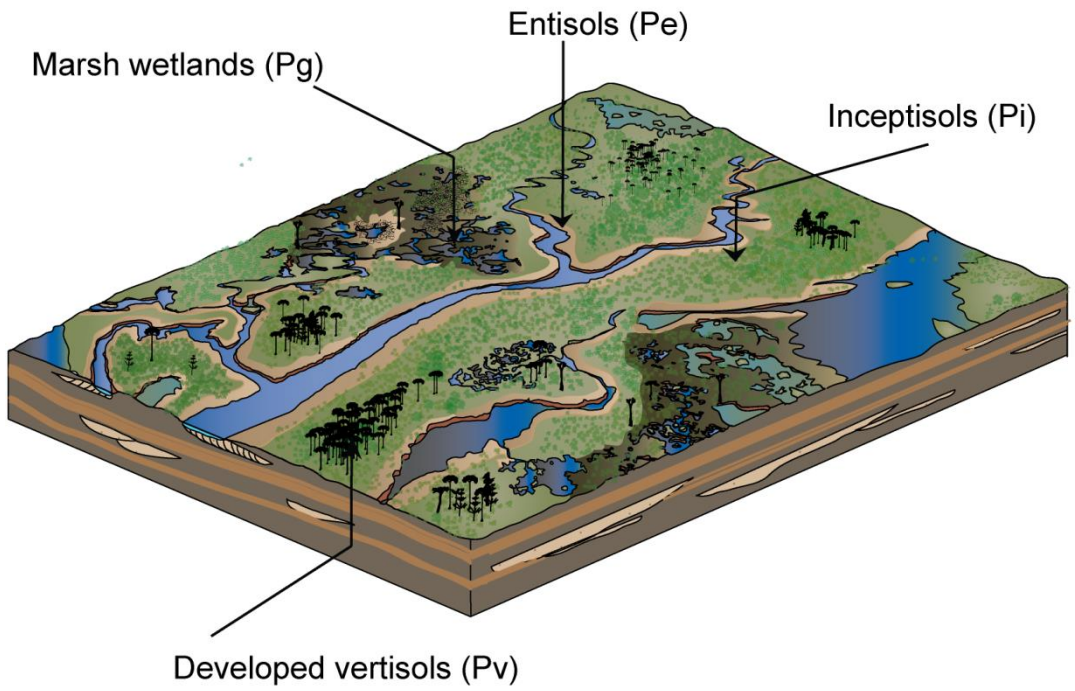
Fig. 11. The thickness of laminated grey siltstones compared with palaeosols graphed in 10 m thickness intervals. If the grey laminated siltstones are deposited in standing bodies of water this plot can be used as a proxy for the position of the watertable on the floodplain.
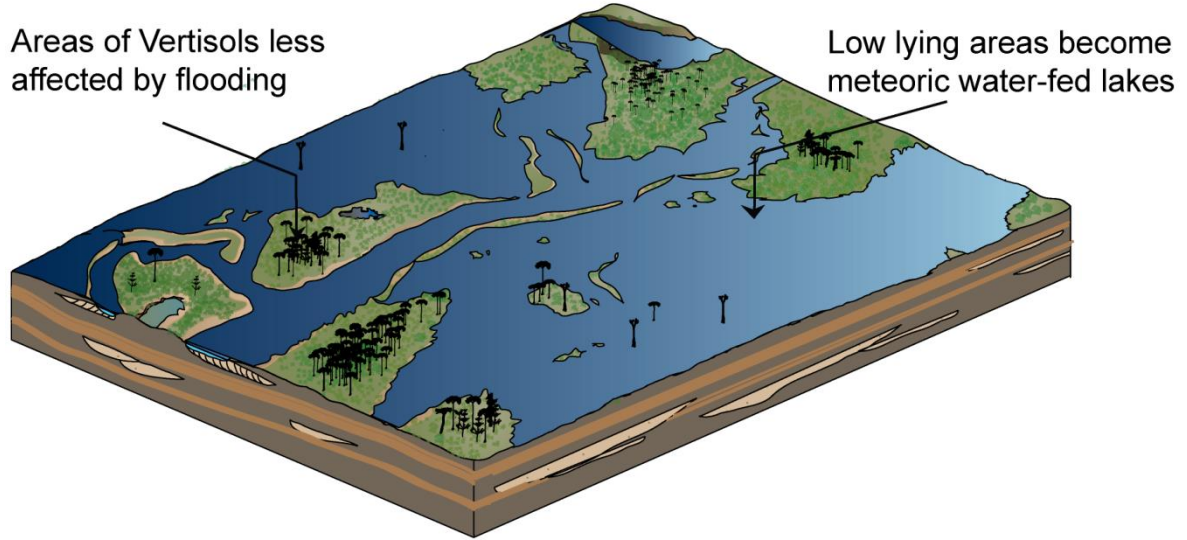
In dry conditions

Marsh wetlands (Pg)

Entisols (Pe)

Inceptisols (Pi)

Developed vertisols (Pv)

In wet conditions

Areas of Vertisols less affected by flooding

Low lying areas become meteoric water-fed lakes

1096

1097　Fig. 12.　A reconstruction of the Ballagan Formation palaeoenvironment in 'dry' conditions
1098　when palaeosols are dominant, and in wet conditions when large bodies of standing water
1099　dominate. Topographically higher areas of vertisols less affected by flooding.